

7-21-2005

High temperature effect of geopolymeric coatings on concretes

Natalya Privorotskaya

Follow this and additional works at: <http://scholarworks.rit.edu/theses>

Recommended Citation

Privorotskaya, Natalya, "High temperature effect of geopolymeric coatings on concretes" (2005). Thesis. Rochester Institute of Technology. Accessed from

This Thesis is brought to you for free and open access by the Thesis/Dissertation Collections at RIT Scholar Works. It has been accepted for inclusion in Theses by an authorized administrator of RIT Scholar Works. For more information, please contact ritscholarworks@rit.edu.

High Temperature Effect of Geopolymeric Coatings on Concretes

by

Natalya Privorotskaya

Advisor Dr. Benjamin Varela

Co-advisor Dr. Amandio Teixeira-Pinto

**A Thesis Submitted in
Partial Fulfillment of the
Requirement for the**

**MASTER OF SCIENCE
IN
MECHANICAL ENGINEERING**

Approved by:

Dr. B. Varela

Department of Mechanical Engineering
Rochester Institute of Technology

Dr. A. Teixeira-Pinto

Department of Civil Engineering
Universidade de Trás-os-Montes e Alto Douro

Dr. A. Langner

Department of Chemistry
Rochester Institute of Technology

Dr. H. Ghoneim

Department of Mechanical Engineering
Rochester Institute of Technology

Dr. E. C. Hensel

Department Head of Mechanical Engineering
Rochester Institute of Technology

Benjamin Varela

(Thesis advisor)

A. Teixeira-Pinto

(Thesis co-advisor)

Andy Langner

Hany Ghoneim

Edward Hensel

Permission granted

High Temperature Effect of Geopolymeric Coatings on Concretes

I, Natalya Privorotskaya, hereby grant permission to the Wallace Library of the Rochester Institute of Technology to reproduce my thesis in whole or in part. Any reproduction will not be for commercial use or profit.

Signature of Author: **N. Privorotskaya**
Date: 7.21.2005

Acknowledgements

My sincere gratitude and appreciation are extended to my advisor, Dr. Benjamin Varela. His scientific excitement, invaluable advice as well as constant support and guidance inspired me to make the right decisions and continue with this research over the course of last two years. I greatly appreciate all of the effort and time that were spent in various laboratories during sample preparation, equipment setup, and testing. Many thanks go to Dr. Amandio Teixeira-Pinto and his assistant, Paulo Osório, for the collaboration, warm welcome, and assistance during my stay and work at the University of Trás-os-Montes and Alto Douro in Portugal. Gratitude is extended to Professors Maureen Valentive and Todd Dunn for allowing the use of Soils and Materials Laboratory in the Civil Engineering Department within Rochester Institute of Technology as this work would not be possible without the use of the appropriate facilities.

Special thanks go to my colleagues, Kunal Shrotri, for his explanation and initial demonstration of the infrared analysis and thermogravimetric equipment, as well as Arthur Deane, for assisting with sample preparation during the first stages of this research work. My appreciation is extended to all of the individuals who ensured smooth and timely completion of the experiments by providing professional advice and dedicating many hours to laboratory testing. This list includes, but is not limited to, Dr. Andreas Langner in the Chemistry Department at Rochester Institute of Technology, who assisted with the interpretation of the infrared results; Dr. Bruce Kahn and Yu Xia at the Center of Materials Science and Engineering at RIT for their help with obtaining scanning electron microscope photographs of geopolymer; Professor Pedro Tavares and Nuno Martins of the University of Trás-os-Montes

and Alto Douro for assistance with the use of SEM as well as infrared analysis of mortar samples; Dr. Beth Carle in Mechanical and Manufacturing Engineering Technology Department at RIT, who provided assistance with setup and operation of compressive testing equipment.

Abstract

Microstructure and thermal properties of inorganic geopolymeric materials synthesized from metakaolin at 65°C have been investigated for their further application as a thermal barrier for concrete structures. Thermogravimetric analysis of two geopolymer compositions revealed good thermal stability of this material at temperatures of up to 1000°C. Substantial expansion of the samples with addition of silica were observed during heat treatment at 450°C and 800°C, accounting for the differences in microstructure between the two compositions as was seen with scanning electron microscope. Infrared analysis revealed the presence of additional structural groups for silica-containing specimens.

The ability of mortar samples to withstand elevated temperatures was based on the degree of compressive strength loss as well as the microstructure changes that were observed before and after the exposure of specimens to 450°C and 800°C for one hour. As compared to unprotected concrete, the reduction in strength at 450°C was 12% and 14% less for mortar cubes coated with metakaolin-based geopolymer and that with addition of amorphous silica, respectively. At 800°C, the observed difference was more than 20%. Infrared analysis and electron spectroscopy studies of heat treated mortar showed little signs of deterioration when samples were coated with geopolymer. Consequently, it was determined that geopolymer can be used as a suitable coating for thermal protection of concrete.

Contents

| | |
|---|-----------|
| Acknowledgements | ii |
| Abstract | iv |
| List of Figures | viii |
| List of Tables | ix |
| 1 Introduction | 1 |
| 2 Work Objectives | 4 |
| 3 Literature Review | 7 |
| 3.1 Concrete | 7 |
| 3.1.1 High Temperature Effects | 8 |
| 3.2 Geopolymer | 11 |
| 3.2.1 Terminology | 12 |
| 3.2.2 Processing and Synthesis | 13 |
| 3.2.3 Properties | 15 |
| 3.2.4 High Temperature and Coating Applications | 18 |
| 4 Sample Preparation and Characterization | 20 |
| 4.1 Geopolymer Preparation | 20 |
| 4.2 Mortar Samples | 22 |
| 4.3 Geopolymer Coated Mortar Samples | 23 |
| 4.4 Sample Characterization | 24 |
| 4.4.1 Geopolymer | 24 |
| 4.4.2 Concrete | 26 |
| 5 Analysis and Discussion | 27 |
| 5.1 Geopolymer Characterization | 27 |
| 5.1.1 Curing Behavior | 27 |
| 5.1.2 Thermogravimetric Analysis | 28 |
| 5.1.3 High Temperature Effects | 31 |
| 5.1.4 Fourier Transform Infrared Analysis | 33 |
| 5.1.5 Scanning Electron Microscopy | 38 |

| | | |
|----------|--|-----------|
| 5.2 | Concrete | 45 |
| 5.2.1 | Thermogravimetric Analysis | 45 |
| 5.2.2 | Compressive Strength Measurements | 46 |
| 5.2.3 | Scanning Electron Microscopy | 51 |
| 5.2.4 | Fourier Transform Infrared Analysis | 58 |
| 6 | Conclusions and Suggestions for Future Work | 63 |
| 6.1 | Conclusions | 63 |
| 6.2 | Future Work | 64 |
| | Appendices | 67 |
| A | Collected Data: Compressive Strength Measurements | 67 |
| B | Scanning Electron Microscopy and Infrared Analysis | 69 |
| | References | 72 |

List of Figures

| | | |
|------|---|----|
| 3.1 | The effect of temperature on the modulus of elasticity strength of different types of concretes | 9 |
| 3.2 | Sialate chain | 12 |
| 3.3 | Geopolymer chemical structure as proposed by Barbosa et al. | 17 |
| 4.1 | Cut-away view of a mold used for coated sample preparation | 23 |
| 5.1 | Thermogravimetric curves for metakaolin-based geopolymer at a heating rate of 10°C/min in oxygen atmosphere | 29 |
| 5.2 | Thermogravimetric curves for metakaolin based material with addition of amorphous silica at a heating rate of 10°C/min in oxygen atmosphere | 29 |
| 5.3 | Cracking of metakaolin-based samples at 450°C and 800°C | 31 |
| 5.4 | Metakaolin/silica sample expansion when subjected to elevated temperatures | 32 |
| 5.5 | Infrared analysis of kaolin starting material | 34 |
| 5.6 | Infrared analysis of metakaolin | 34 |
| 5.7 | Infrared spectrum of metakaolin-based (MK) geopolymer | 35 |
| 5.8 | Infrared spectrum of silica | 36 |
| 5.9 | The structure of lone silanol | 37 |
| 5.10 | Infrared spectrum of metakaolin-based geopolymer with addition of amorphous silica (MKS) | 37 |
| 5.11 | SEM micrograph of metakaolin-based geopolymer | 38 |
| 5.12 | SEM micrograph of metakaolin-based geopolymer with addition of silica . . | 39 |
| 5.13 | Cracking of metakaolin-based geopolymer at room temperature as revealed by SEM | 40 |
| 5.14 | Cracking of metakaolin-based geopolymer at 450°C as revealed by SEM . . . | 41 |
| 5.15 | Surface of metakaolin-based geopolymer with addition of silica at 450°C and 800°C as revealed by SEM | 42 |
| 5.16 | Cracking of metakaolin-based geopolymer with addition of silica at 450°C and 800°C as revealed by SEM | 44 |
| 5.17 | Thermogravimetric curves for mortar sample at a heating rate of 10°C/min in oxygen atmosphere | 45 |
| 5.18 | Compressive strength of unprotected mortar cubes (control group) in the range of 25-800°C | 47 |
| 5.19 | Compressive strength of mortar cubes coated with metakaolin-based geopolymer in the range of 25-800°C | 48 |

| | | |
|------|--|----|
| 5.20 | Compressive strength of mortar cubes coated with silica-containing metakaolin-based geopolymer in the range of 25-800°C | 49 |
| 5.21 | Trend of compressive strength loss over the 25-800°C temperature range for unprotected, MK-, and MKS-coated mortar cubes | 50 |
| 5.22 | Micrograph of cured mortar | 51 |
| 5.23 | Mortar microstructure after exposure to 450°C | 52 |
| 5.24 | Mortar microstructure after exposure to 800°C | 53 |
| 5.25 | MK-coated mortar microstructure after being exposed to 450°C | 54 |
| 5.26 | MK-coated mortar microstructure after being exposed to 800°C | 56 |
| 5.27 | MKS-coated mortar microstructure (interior) after being exposed to 450°C and 800°C | 57 |
| 5.28 | Infrared spectrum of unheated concrete | 58 |
| 5.29 | Infrared spectra of concrete exposed to 450°C and 800°C | 60 |
| 5.30 | Infrared spectra of MK-coated concrete exposed to 450°C and 800°C | 61 |
| 5.31 | Infrared spectra of MKS-coated concrete exposed to 450°C and 800°C | 62 |
| B.1 | Scanning electron microscope (SEM) micrographs of unprotected (a), (b), (c), MK-coated (d), (e), and MKS-coated (f), (g) mortar microstructure at room temperature and after exposure to 450°C and 800°C | 70 |
| B.2 | Infrared (IR) spectra of unprotected (a), (b), (c), MK-coated (d), (e), and MKS-coated (f), (g) mortar at room temperature and after exposure to 450°C and 800°C | 71 |

List of Tables

| | | |
|-----|--|----|
| 3.1 | Geopolymer designations as proposed by J. Davidovits | 13 |
| 3.2 | Properties of geopolymers with Al/Si ratio of approximately 2 | 15 |
| 4.1 | Chemical composition of starting materials | 20 |
| 4.2 | Sample preparation proportions | 22 |
| 5.1 | Weight loss of samples after curing and exposure to 450°C and 800°C | 27 |
| 5.2 | Percent original strength retained by the mortar after exposure to 450°C and 800°C | 50 |
| A.1 | Compressive strength (psi) of Unprotected, MK-, and MKS-coated mortar cubes at room temperature, 450°C and 800°C | 68 |

Chapter 1

Introduction

Concrete is a combination of cement, aggregates, and water chemically mixed together and cured to result in a material that is well suited for construction purposes [1]. Cements have been used in construction industry since Egyptian and Roman times, while concrete dates back to 1800s. It gained its popularity as a building material due to a combination of favorable properties, such as high compressive strength, reasonable durability, ease of handling, and low production cost [2]. Moreover, concretes can be reinforced or prestressed to fit a wide variety of applications [1]. Presently concrete is used for such structural applications as bridges, dams, buildings, arches, and roofs [3].

Although concrete is widely used in construction industry, it has been found that there is a set of limitations associated with it. Some weaknesses, such as low resistance to acid and sulfate attack, carbonation, and slow alkali-silica reaction, are related to the chemical composition of the material. Production techniques, which can not be altered, require high energy consumption and have a negative environmental impact. Carbon dioxide gas, which is a byproduct of concrete manufacturing, contributes to the greenhouse effect and consequently global warming [4][5]. The degradation of mechanical properties is the biggest problem associated with concrete as it is usually used as a load bearing structure. It has been found that concrete does not maintain its compressive strength when subjected to temperatures higher than 400°C [6][7]. Moreover, large cracks may develop as a result of heat exposure, leading

to the permanent loss of durability, structural stability, and subsequent failure. Temperature rise can be observed under conditions involving large amounts of energy release, such as in nuclear plants and fires.

Several strategies may be employed to prevent deterioration of concrete when it is subjected to elevated temperatures. For example, its composition can be altered to yield a material with more favorable properties or it can be insulated on the heated side [8]. Since changing concrete's composition is not feasible for an existing construction, coating concrete with a protective layer is considered. Such material should not only possess high thermal stability, but should also be fairly inexpensive and easily manufactured if it is to be incorporated into the mass production. Most organic polymers cannot be used for such purposes since they soften and ignite at temperatures of 400-600°C. Carbon and glass fibers are suitable for high temperature applications, but high temperature fiber binding matrix is not available at the present time [9].

This work considered geopolymer, an inorganic polymeric material based on silicon and aluminum, as a possible coating for concrete. An increase in the use of geopolymers can be attributed to the widespread availability of raw materials, ease of production, and the ability to manipulate their mechanical, chemical, and thermal properties by altering chemical composition. Since all of its constituents are available commercially and often consist of waste materials, geopolymers are easy and inexpensive to manufacture. In addition, they can be fabricated and cured at ambient temperature. Production of geopolymers requires lower levels of energy consumption than those needed for concrete. Moreover, geopolymer manufacturing does not produce harmful CO₂ gases that can be viewed as one of the greatest disadvantages of cement production industry [10].

Geopolymer's properties can be tailored for specific applications by changing concentrations of initial starting materials or including certain types of aggregates. Si/Al ratio was found to play an important role in determining mechanical and thermal characteristics associated with geopolymers. Previous tests showed that unlike other materials, geopolymer may

be stable up to 1300°C [11], making them perfect candidates to be used for thermal protection of concrete structures. Such applications may include, but are not limited to, fire-prone construction buildings, nuclear plants, and other structures subjected to high temperature environments.

Chapter 2

Work Objectives

The objective of this work is to investigate the potential use of geopolymeric materials as the coating for concretes in high temperature applications. In order to determine whether these material can serve as a suitable thermal barrier in concrete structures, its behavior over 25-800°C temperature range was analyzed. Characterization of samples was necessary to gain better understanding of geopolymer thermal behavior. Two compositions with varying Si/Al ratios were considered for this analysis. The first configuration is metakaolin-based (designated MK) with Si/Al ratio of approximately 2. Metakaolin-based samples with addition of silica (designated MKS) comprised the second set of specimen. Their composition corresponded to Si/Al ratio of 6.

The following tests were conducted in order to characterize prepared geopolymeric samples:

1. Thermogravimetric analysis (TGA) was performed to monitor the effect of increasing temperature on the thermal stability of geopolymer samples.
2. Infrared analysis was used to determine functional groups present in the samples after their synthesis. In particular it was employed to establish the kinds of molecular structures within the material. This approach was useful in following the changes that occur when altering starting reagents and their proportions.

3. Scanning electron microscopy (SEM) study was conducted to reveal geopolymer microstructure. Observed differences were related to the material behavior and its properties. This technique can provide information about microstructure changes that occur upon heat treatment of geopolymer samples.

The results obtained from the testing of geopolymers was applied to determine whether geopolymer can be used as a suitable coating to protect concrete from elevated temperatures. Both quantitative and qualitative analysis were performed by means of observation and experimentation. Geopolymer was applied to mortar cubes as described below in order to demonstrate high temperature application of this new material. The following procedure outlines the steps taken in reviewing the effectiveness of geopolymer coatings.

1. Apply metakaolin-based polymer to mortar cubes. Mortar specimen are covered with 0.25" thick geopolymer coating and cured at 65°C as described in *Sample Preparation* Section.
2. Expose the resulting samples to 450°C and 800°C for one hour. These temperatures were chosen based on the extensive literature search presented in *Literature Review* Section of this work. Concrete was shown to deteriorate starting at 400°C and lost most of its original compressive strength at 800°C.
3. Test coated and unprotected mortar samples for compressive strength to determine whether geopolymer offers any thermal protection to concrete and to what degree. The effects were quantified based on the percentage of strength lost after heating the specimen.
4. Conduct Fourier Transform Infrared (FTIR) analysis on protected samples and compare the results to those seen for the unprotected mortar. This will provide a sense of chemical changes occurring within the specimens as a function of temperature and geopolymer coating.

5. A scanning electron microscopy study was performed to record microstructural changes in concrete. The test was carried out on all heated specimens in order to compare microstructure across the samples. Photographs were made on the exterior surface of the mortar cube as well as of its interior portion to track microstructural changes as a function of distance from the heat source.
6. Repeat procedure in 1–5 above using geopolymer with higher Si/Al ratio.

A recommendation on using geopolymers for thermal protection of concrete is made. The reasons for choosing a certain chemical composition for the polymer are described in detail.

Chapter 3

Literature Review

Numerous studies on the properties of concrete and geopolymer have been done in the past decades. An evaluation of changes in concrete properties as a function of temperature is presented and proposed solutions for maintaining thermal stability of the material are considered. Geopolymeric materials are then examined as an alternative way to prevent or reduce concrete deterioration. Their insulating properties as reported by researchers in the field are explored to serve as the basis for further discussion.

3.1 Concrete

After the collapse of the World Trade Center in September 2001, Federal Emergency Management Agency (FEMA) conducted a study concerning building performance [12]. Fire protection of concrete and steel structures was one of the main concerns addressed in this study. FEMA's report emphasized the inadequacy of current fire standards as they rely on laboratory testing. Most laboratories are unable to accommodate real-size structural members. Consequently, the results that they provide should be used solely for comparative purposes rather than as a deciding factor in engineering design and evaluation of structural performance.

Protecting concrete's structural stability at elevated temperatures may be useful in case of fires as it would allow more time for emergency evacuation. A survey conducted by National Institute of Standards and Technology (NIST), revealed that out of 22 cases recorded between 1970 and 2002 seven building destructions and total collapses occurred in concrete structures [13]. Fire, usually uncontrolled for a prolonged period of time, was the cause of all of these documented accidents. If the appropriate protective measures are taken, the structure may obtain only minimal damage and consequential repairs would be unnecessary. On the other hand, if concrete is not protected, it would deteriorate much quicker, creating dangerous environments. Such situation occurred in July of 2001 during the fire inside the tunnel in Baltimore, Maryland caused by the derailment of the train carrying liquid tripropylene [14]. The tunnel surface wall temperatures reached approximately 800°C, resulting in severe damages.

Concrete is one of the most widely used materials in construction. It can support large loads and carries significant stresses when those loads are applied. Since concrete's mechanical and thermal properties largely depend on raw materials and their relative proportions, as well as porosity and the age of concrete, it is important to provide a comprehensive review of studies on the evaluation of concrete performance under high temperature conditions.

3.1.1 High Temperature Effects

As was mentioned previously, concrete does not perform well at elevated temperatures. Water evaporation from concrete results in large amounts of shrinkage within the material [15], which in turn causes cracking and spalling [6][16][17]. Moreover, evaporation of constituent water from concrete results in the loss of structural integrity, strength loss, reduced ability to withstand impacts, carry loads and may cause structural collapse. Volume changes can also be attributed to the chemical dissimilarities between the cement and aggregates that are combined during concrete production [15]. Some of the constituents, such as quartz and calcium carbonate, polymerize or undergo chemical transformations with added

heat, resulting in nonuniform shrinkage and expansion. Having different coefficients of thermal expansion, concrete constituents are thermally incompatible. Voids are produced upon temperature rise. According to Li et al. [6] and Poon et al. [7], these changes become noticeable around 400°C. They are revealed as a substantial strength loss and subsequent collapse of the structure. El-Hawary et al. reported a decrease in modulus of elasticity and shear modulus with temperature increase [18]. FEMA study on structural stability pointed out that concrete loses half of its original modulus of elasticity at 400°C as indicated in Figure 3.1 [12].

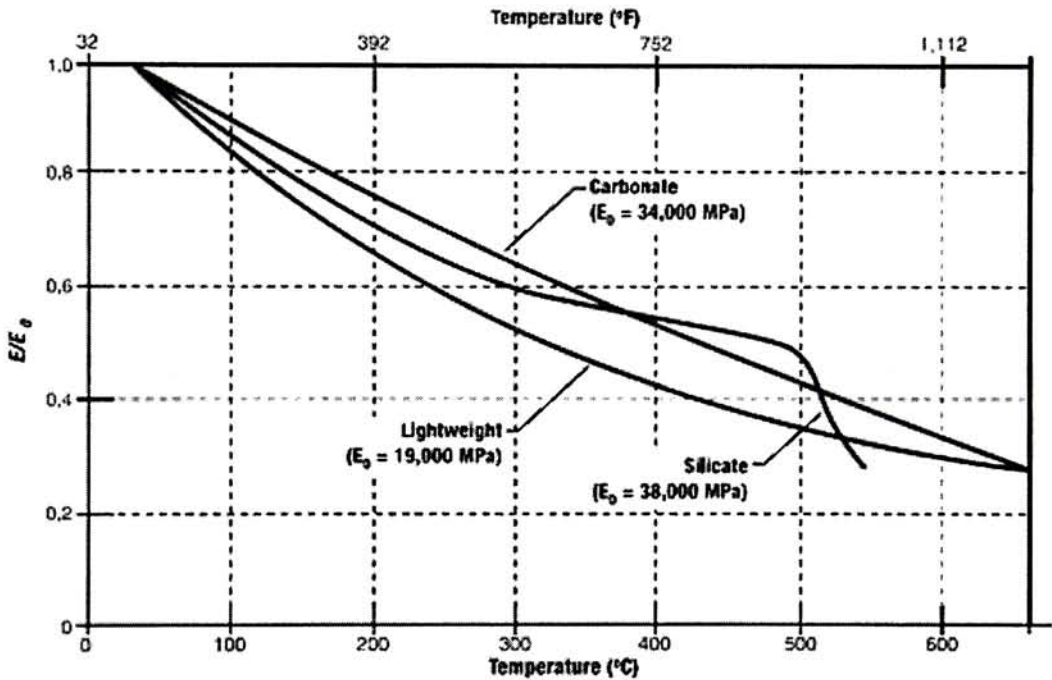


Figure 3.1: The effect of temperature on the modulus of elasticity strength of different types of concretes

Weigler and Fischer reported that about 80% of the original strength is maintained if the specimen is heated to no more than 300°C [19]. By the time concrete reaches 600°C, about 46-79% of its strength is gone, as compared with 7-21% remaining after 800°C [7][17], depending on initial composition. It is a common practice to consider 600°C as the temperature beyond which concrete is no longer structurally sound [17]. Since concrete is one of

the most popular construction materials and plays an essential role in protecting steel from elevated temperature in reinforced concrete, some form of protection is necessary to shield the exposed surface of concrete from the heat.

Some of the compressive strength of concrete can be recovered through post-fire-curing process. The process, examined by Poon et al. [7], is based on the rehydration of the cement grains and lime contained in the concrete mixture. Experiments showed that water-recured normal strength concrete specimen regained 61-85% and 31-56% of their original strength after being subjected to temperatures of 600°C and 800°C, respectively. Air-recuring is also possible but is 15-20% less effective than that done in water environment. Overall, this technique is not very efficient for concretes subjected to temperatures of 500°C and higher, as large cracks that can not be refilled are developed at above-mentioned temperatures. In addition, constant moisture supply is necessary to expedite the recovery process and to ensure that the strength is regained to the maximum extent. This may prove to be cost prohibitive for large structures. More importantly, such an action is not realistic for real-world stress-bearing structures due to their large sizes and the need for immediate support after the fire as concrete would be unable to withstand developed stresses.

Since repairing concrete microstructure after material has been subjected to elevated temperatures is not efficient and may be quite expensive, other ways of protecting it are necessary. Most studies concentrate on combining aggregates in such proportions as to obtain greater thermal stability. Furthermore, other components may be incorporated into the mix in addition to standard ingredients used. These additives act to increase specific heat and decrease thermal diffusivity and thermal conductivity of the concrete in order to improve its insulating capabilities [20]. A high value of specific heat is desired as it represents the amount of heat required to raise the temperature of the material by one degree Celsius. At the same time, low thermal conductivity and diffusivity are indicative of the material that is not easily influenced by the temperature changes in the surrounding environment.

In a study conducted in Korea, an evaluation of basaltic concrete at high temperatures showed that a reduction of thermal conductivity of more than 40% and 53% occurs at 500°C and 900°C, respectively. Similarly, thermal diffusivity values decreased by 49% at 500°C [21]. Such level of thermal stability can be achieved by introducing various additives into the concrete mix. For example, Xu and Chung [20] found that an addition of silica fume reduces thermal conductivity by about 34%, while Kim et al. [22] reported a reduction of 33% when cement is completely replaced with slag. The addition of silica fume also increases the value of the specific heat [20].

3.2 Geopolymer

Geopolymer is an inorganic polymeric material, also known as polysialate, which consists primarily of silicon, aluminum, oxygen, sodium or potassium, and water [4]. It belongs to the class of amorphous aluminosilicates that can be cured at ambient temperature and atmospheric pressure. These materials were first recognized by V.D. Glukhovskiy as "soil cements". He claimed that in ancient concretes, substances derived from the reaction of aluminosilicates with high pH alkaline solutions exhibited superior properties due to the coexistence of calcium silicate hydrate (C-S-H) and alkaline aluminosilicate hydrate. The latter material represents an impure form of what is now known as geopolymer [23].

Beginning in 1970s, French chemist Joseph Davidovits examined the chemical structure of alkali activated aluminosilicates and introduced the term geopolymer as a conventional name for these materials. The main purpose of geopolymers was to replace other conventional plastics and cements that would easily ignite and burn at relatively low temperatures, with a material of greater thermal stability. One of the first uses of geopolymers was in the manufacturing of sintered weatherproof panels [24]. Davidovits and his co-workers further advanced the field of geopolymers in the 1980s by developing mineral polymers called polysialates that could be polymerized at temperatures of up to 120°C [25]. Davidovits became one of the

leading investigators in the field of geopolymeric materials, opening Cordi-Geopolymere, a company specializing in geopolymer research and development.

As shown by the previous research [4][11], geopolymer's strength, hardness, thermal diffusivity and conductivity highly depend on composition, especially silicon to aluminum ratio. Consequently, its properties can be altered to fit specific application requirements. According to Barbosa et al., in contrast to concrete, geopolymers perform well under temperatures as high as 1300°C [11]. Thus, geopolymer may be a suitable material to create a thermal barrier between exposed concrete and its environment.

3.2.1 Terminology

Polysialate, an abbreviation for silicon-oxo-aluminate [5], is a designation that was suggested for the chemical structure of geopolymer. Sialate is a chain of silicon and aluminum tetrahedrons that are bonded together through shared oxygen bridges [26] as shown in Figure 3.2. According to the Loewenstein's aluminum avoidance principle, two aluminum molecules

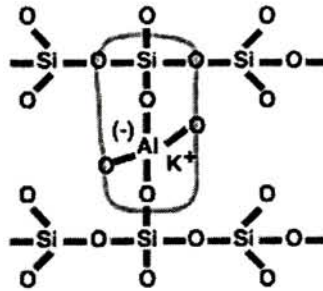


Figure 3.2: Sialate chain

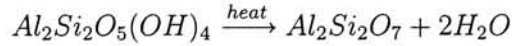
cannot be bonded together by an oxygen [5]. Thus, an aluminum tetrahedron has to be linked to a silicon molecule, limiting the number of obtainable chemical structures. In order to differentiate between various combinations of these molecules, geopolymers are divided into several groups according to chemical structure units that they form. Some of the basic designations are as follows [11]:

| Unit Name | Chemical Structure | Designation |
|------------------|-----------------------|-------------|
| Sialate | -Si-O-Al-O- | PS |
| Sialate siloxo | -Si-O-Al-O-Si-O- | PSS |
| Sialate disiloxo | -Si-O-Al-O-Si-O-Si-O- | PSDS |

Table 3.1: Geopolymer designations as proposed by J. Davidovits

3.2.2 Processing and Synthesis

Most of the raw materials used for geopolymer formation are of geological origin or by-product materials. Many common minerals, such as clays and granites are good sources of aluminosilicates [27]. Fly ash, a by-product of coal combustion, is also rich in silicon and aluminum and can be used as a base for geopolymer formation. Silicates are found in abundance in kaolin, a natural material rich in kaolinite ($\text{Al}_2\text{Si}_2\text{O}_5(\text{OH})_4$) [11][28]. When kaolin is exposed to temperatures in the range of 450-750°C, it undergoes a series of chemical transformations. The following dehydration reaction results in a material known as metakaolin ($\text{Al}_2\text{Si}_2\text{O}_7$).



Granizo et al. [29] established that the thermal treatment of kaolin at 750°C for 24 hours yields its complete dehydroxilation. However, according to the XRD, FTIR, and MAS-NMR, the same results can be achieved in as little as 2-10 hours, as reported by other researchers [11][30][31]. The final atomic structure of metakaolin is such that it does not rehydrate in the presence of water [28].

Unlike kaolin, metakaolin is X-ray amorphous and highly reactive in the alkaline environment [4][29]. Geopolymers are synthesized in the presence of alkaline ions under high pH conditions that force dissolution of silicon and aluminum [20]. Further polymerization yields gel-like material with the following empirical formula:

$$M_n\{(\text{SiO}_2)_z(\text{AlO}_2)\}_n, w\text{H}_2\text{O}$$

where M is a positive cation, such as sodium or potassium, z is 1, 2, or 3, n is the degree of polycondensation, and w is the mole number of hydrated water (usually up to 7) [25]. Geopolymerization starts immediately upon mixing of the initial materials and continues until complete curing has been reached [32]. Na^+ , K^+ , or other positive ions are necessary for synthesis in order to cancel the overall negative charge associated with a four-coordinated Al^{+3} present in the basic structure of geopolymer [26]. In general, prefix M- is used with the polysialate unit designation, where M represents alkaline ion as described above [5].

Although geopolymerization is not yet fully understood, it is believed that it involves two steps: dissolution and polycondensation. Babushkin et al. proposed a scheme representing the possible chemical process for the dissolution of Al-Si minerals under strongly alkaline conditions [20][33]. Studies showed that polymerization process greatly depends on the concentrations of starting materials as well as their relative proportions, temperature, and time of reaction [20][29][34]. As expected, the rate of geopolymer formation increases with temperature, sometimes making it difficult to attain uniform mixture due to the unintended formation of clusters rather than smooth slurry [35]. Reaction degree increases with increased activator concentration [29]. However, there exists a critical liquid/solid ratio beyond which metakaolin no longer forms new polymer, but falls out as precipitant instead. Water, aluminum, and silicon content were shown to be critical for the proper hardening of the geopolymer [11]. In their research, Barbosa et al. polymerized seven geopolymers with various $\text{SiO}_2/\text{Al}_2\text{O}_3$, $\text{Na}_2\text{O}/\text{SiO}_2$, and $\text{H}_2\text{O}/\text{Na}_2\text{O}$ ratios in the presence of sodium alkaline ions [11][36]. It was shown that geopolymer attains best mechanical properties when the Si/Al ratio is equal to 2. This composition yielded a material that could be cured at temperatures not exceeding 65°C and had a compressive strength of 48.1 MPa. This research group also reported slow curing of samples with high water content even at elevated temperatures, which, in turn, resulted in poor compressive strength and hardness.

3.2.3 Properties

Most of the early work associated with geopolymeric use in high temperature environments targeted industrial applications rather than academic research [5]. Therefore, the majority of information available on chemical structure and preparation of geopolymers comes from patent literature [24][25][37]. Early work related to geopolymers was concentrated on manufacturing of sintered panels that utilized silico-alkaline mixtures to achieve fire-proof material [24].

Table 3.2 lists properties that are commonly associated with geopolymers. These properties were obtained through experimental results, which means that they may vary if different starting materials, concentrations, and sample preparation techniques are used.

| Property | Reported Value |
|---------------------------|---|
| Compressive Strength [11] | 48.1 MPa |
| Thermal Diffusivity [4] | $225 \times 10^{-8} \text{ m}^2/\text{s}$ |
| Thermal Conductivity [4] | 3.17 W/m·K |
| Specific Heat [4] | 1.085 kJ/kg·K |
| Density [4] | 1300 kg/m ³ |

Table 3.2: Properties of geopolymers with Al/Si ratio of approximately 2

Research showed that geopolymer achieves its optimum mechanical properties when there is enough alkali ions for all the constituents to react completely. The excess of Na^+ ions results in high concentration of sodium silicate due to incomplete polymerization. During the drying stage, sodium migrates to the surface, forming sodium carbonate when it reacts with carbon dioxide in the atmosphere. Fourier Transform Infrared Radiation (FTIR) testing revealed that in this case the charge is not properly balanced throughout the material. The resulting polymer lacks in both strength and hardness [36].

Attainable strength of geopolymer also depends on the order in which raw materials are mixed, as was demonstrated by the research conducted in Madrid, Spain by A. Palomo et al. [38]. It was found that mixing the alkaline solution with sodium silicate and then adding metakaolin results in smaller compressive strength than if sodium silicate is added to an

alkaline solution and metakaolin mixture. The authors attributed this behavior to the rate of the formation of geopolymer, which was higher in the first case than in the second.

The curing time of geopolymer is not only a function of initial constituents, but also depends on the environmental conditions, such as humidity and temperature. The setting can take anywhere from 24 to 48 hours [10]. However, in his patent on polysialate, Davidovits reported curing times of 30 minutes to as long as 15 hours [25]. Unlike other polymeric materials, geopolymer can be cured at room temperature. This property makes it very attractive for the manufacturing industry as no additional processes or equipment would have to be involved, greatly diminishing the costs associated with production. In order to accelerate the setting of the polymer, it can be cured in an oven at relatively low temperatures of 65-90°C. Curing times can be shortened significantly if additional sources of heat are used during the drying stage. Geopolymers that result in good mechanical properties have a fairly short setting time due to the large alumino-silicate to alkaline solution ratio [20]. This is achieved by reacting large percentage of metakaolin in high pH environment [34].

As revealed by the X-ray diffraction [5][11], geopolymers can be either semi-crystalline or amorphous. The degree of crystallinity depends on the curing conditions, such as moisture contents, and initial concentrations of starting materials [32]. The experimental work done by Barbosa showed that all geopolymer samples exhibit glassy structure regardless of the curing temperature [11]. Figure 3.3 shows a model of the proposed structure that takes into consideration voids necessary for metal ions and water. Together with water, positive ions are trapped in the voids between silicon and aluminum tetrahedrons [32]. This structure was somewhat revised from that proposed by Davidovits [39] to better fit experimental data.

Oftentimes structural applications require the material in question to have good shape and size stability under various environmental conditions. Dilatometry analysis showed that geopolymer remains dimensionally stable in the temperature range between ambient and 1000°C [36]. Small amount of shrinkage occurs between 250°C and 800°C due to the water loss and continues until 880°C due to the volume changes resulting from crystallization.

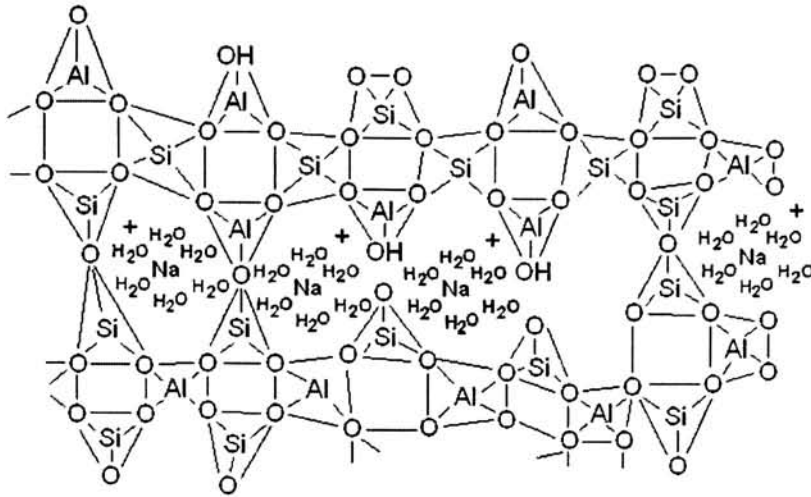


Figure 3.3: Geopolymer chemical structure as proposed by Barbosa et al.

As can be seen from Table 3.2, geopolymers are characterized by low values of thermal diffusivity and thermal conductivity. In comparison, coefficients of thermal conductivity for other conventional building materials, such as steel, are as much as 15 times greater [4]. Low values are representative of the insulating materials that can withstand high temperatures without significant negative effects on their compressive strength. These properties make geopolymers perfect candidates for use at elevated temperatures or in the environment with large temperature differentials.

Palomo et al. conducted quenching experiments on geopolymeric material in order to gain a better understanding on how its properties change as temperature increases [38]. The group concluded that geopolymer undergoes microstructural transformations upon losing water. Further changes occur starting at 750°C and continue up to 1050°C. These changes also register on infrared spectrum as an additional peak at 515-520 cm^{-1} , corresponding to the formation of crystalline nepheline (NaAlSiO_4). Geopolymer remains in its solid state up to 1300°C, at which point it transforms into molten phase.

3.2.4 High Temperature and Coating Applications

Previously, several attempts to utilize geopolymers as high temperature resistive materials were made. In 1976 J. Davidovits proposed a method of fabricating sintered panels by applying a layer of silico-alkaline mixture followed by a mixture of organic or mineral particles, such as wood, which were then compressed and brought to a temperature of 80°C [24]. He noted that the obtained product was characterized by good response to temperature changes.

Research conducted at Rutgers University in conjunction with the Federal Aviation Administration (FAA) attempted to use carbon fiber reinforced geopolymer-based composites for fire resistance and containment for the aerospace industry [26]. The purpose of the study was to create a material that could withstand 50kW/m² heat flux while preventing the fire from spreading into the cabin, consequently reducing the number of deaths associated with aircraft fire accidents. Conducted experiments indicated that after an exposure of the composite to approximately 1500°F for several hours, the material maintained 63% of its original flexural strength, while the materials currently used in aircraft industry tended to burn, release smoke, and were completely destroyed due to fire exposure.

The geopolymeric material studied by Lyon et al. for the purpose of developing a fire-resistant composite for marine, aviation, and transportation industries was potassium aluminosilicate with the empirical formula $\text{Si}_{32}\text{O}_{99}\text{H}_{24}\text{K}_7\text{Al}$ [9]. An unconstrained expansion of the material was noticed during thermogravimetric testing at temperatures greater than 250°C. Such expansion was attributed to the dehydration reaction that produced steam whose volume was significantly greater than that of the evaporating liquid. Fire calorimetry studies showed that geopolymer-based composites did not ignite or release any appreciable amount of heat and smoke. Their increased fire endurance as compared to other construction and transportation materials means that geopolymers can be used for high temperature applications and where combustion resistance is required.

Barbosa et al. studied the behavior of potassium polysialate (K-PS) and potassium sialate disiloxo (K-PSDS) at temperatures of up to 1400°C [40]. In the case of K-PS sample, they observed surface microcracking and high thermal stability. These samples did not melt after being exposed to 1400°C for one hour and were fully crystallized at the time of reaching 1000°C. On the other hand, K-PSDS polymer with higher Si/Al ratio (3:1 as opposed to 1:1 in K-PS geopolymer) did not crystallize fully and amorphous structure typical of geopolymers was observed at 1400°C. At this temperature K-PSDS sample became porous, losing its dimensional stability. Consequently, it can be concluded that samples with the low value of Si/Al ratio have greater thermal stability and may prove to be useful for thermal protection applications.

Donaldson et al. [32] conducted a preliminary study on the influence of temperature variation with thickness of the material. It was noted that the curing rate may be a function of specimen thickness and must be considered if geopolymer is used for coating applications in order to let the bottom layer to set before any additional layers are applied. Temperatures between 25°C and 60°C were analyzed as they approximated the ambient room and oven curing temperatures. Both experimental results and theoretical calculations showed that the temperature differential across the thickness is insignificant for samples as thick as 30 mm due to the relatively slow curing rate of the polymer at ambient conditions.

Chapter 4

Sample Preparation and Characterization

4.1 Geopolymer Preparation

Metakaolin-based geopolymer (MK) was synthesized from heat-treated kaolin, 15 molal sodium hydroxide solution, and sodium silicate solution. Metakaolin was obtained through dehydroxilation of kaolin at 750°C for 24 hours. The chemical composition of the kaolin (ECC International) is presented in Table 4.1. Sodium hydroxide solution was prepared from NaOH pallets (Acros Organics) dissolved in distilled water. Commercially available STAR

| Components, % mean | Kaolin | Sodium Silicate |
|--------------------------------|--------|-----------------|
| SiO ₂ | 49.0 | 26.5 |
| Al ₂ O ₃ | 36.0 | - |
| Fe ₂ O ₃ | 0.75 | - |
| TiO ₂ | 0.02 | - |
| CaO | 0.06 | - |
| MgO | 0.30 | - |
| K ₂ O | 1.85 | - |
| Na ₂ O | 0.10 | 10.6 |
| P ₂ O ₅ | - | - |
| Loss on ignition | 12.0 | |

Table 4.1: Chemical composition of starting materials
[41][42]

sodium silicate solution supplied by the PQ Corporation with the composition presented in Table 4.1 was used. The reagents were vigorously mixed in proportions outlined in Table 4.2 until a uniform slurry was attained. The mixture acquired a great level of viscosity as soon as the reagents were combined, making it difficult to produce uniformity. Such behavior was previously reported in the literature as well [35]. In order to facilitate the process, metakaolin was added to the activator, formed by combining sodium hydroxide and sodium silicate. As was described in the *Literature Review* chapter of this work, the order in which the starting materials are mixed influences the attainable compressive strength of the geopolymer. However, this research was not concerned with achieving maximum strengths, but rather to show that such material is thermally stable at high temperatures and can be used as a coating to protect concrete from heat exposure.

The obtained mixture was then placed into a 2 x 2 x 1 rectangular mold and cured in Quincy Lab Model 20GC lab oven for 90 minutes at 65°C. The moisture was retained in the samples during the curing process by sealing the top of the mold with plastic film. Samples were left covered in the mold until further testing to ensure that retained water did not evaporate from the surface.

Metakaolin/amorphous silica samples (MKS) were made in a similar fashion, but with an addition of powdered silica (refer to Table 4.2 for proportions). Amorphous silica was obtained from commercial cat litter, which was heated at 450°C for 3 hours. This was done in order to eliminate aromatic compounds present in the product. The resulting material was crushed to powder form. Particles of 300 μ m or less were used for sample preparation. The silica-containing mixture was poured into the same size molds as the MK polymer, covered with thin plastic film, and cured for 4 hours at 65°C. Upon the removal from the oven, samples were left at ambient temperature and pressure for two more hours before being removed from the molds. Specimens were kept covered with plastic film at all times prior to testing to prevent water evaporation.

| Reagent, % by weight | MK | MKS |
|----------------------|------|------|
| Sodium Hydroxide | 18.3 | 18.3 |
| Sodium Silicate | 36.7 | 36.7 |
| Metakaolin | 45 | 27 |
| Amorphous Silica | - | 18 |

Table 4.2: Sample preparation proportions

A set of geopolymer MK and MKS samples were exposed to 450°C and 800°C in a Barnstead/Thermolyne 48000 high temperature furnace in order to analyze temperature response and track changes that occur with an addition of heat. These specimen were removed from the oven one hour later and cooled to the ambient temperature before being tested.

4.2 Mortar Samples

Mortar cubes were prepared according to ASTM C109/C109M test procedure [43] in the Civil Engineering Technology Department at Rochester Institute of Technology. One part of Portland Type I cement was mixed with 2.75 parts of sand and 0.475 parts of water by weight. The resulting mixture was tamped into 2-inch cube molds. Specimens were covered with plastic film and cured at room temperature and standard humidity for at least 3 days before being tested.

All measurements made during the experiments were based on the compressive strength of prepared mortar samples. Consequently, it was critical to maintain uniform mortar composition in order to achieve the same compressive strengths and establish a common baseline for the experimental measurements. It was unnecessary for the concrete to have an optimal compressive strength. Thus, constituents that were readily available in the laboratory, rather than special materials were used to prepare mortar samples.

Specimens were heated to 450 and 800°C. These temperatures were based on data collected from actual electric and hydrocarbon fires as reported in literature [7]. Mortar cubes were cooled back to room temperature by natural convection before being tested.

4.3 Geopolymer Coated Mortar Samples

Mortar cubes were covered on all sides with 0.25-inch thick geopolymeric mixture prepared as described above. In order to achieve uniform coating, special molds had to be fabricated first. The molds were made from two pieces of polyethylene that were glued together, as seen in Figure 4.1. This was necessary to ensure that the molds could be taken apart, and would thus be reusable. In addition, this kind of mold provided repeatable and accurate results. Polyethylene was used as a material of choice because geopolymer has a tendency to bind to other common materials, which would hinder its reuse in the future.

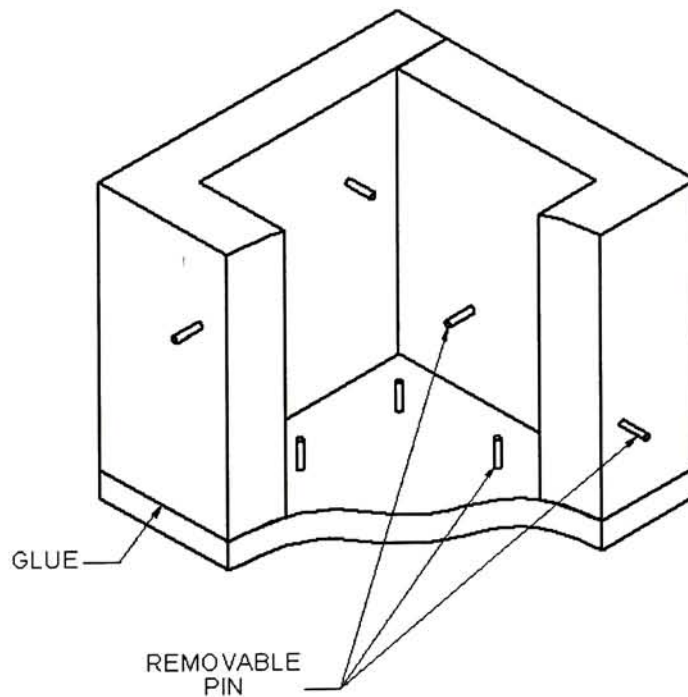


Figure 4.1: Cut-away view of a mold used for coated sample preparation

Four metal pins were inserted into the bottom of the mold and two more on each of the four side. Pins protruded exactly 0.25 inches into the mold cavity to ensure that the mortar cube was centered and covered with geopolymer coating of uniform thickness on all sides. Once the required geopolymer mixture was prepared and the mold was sealed with hot glue,

the cavity of the mold was filled approximately half way with the mixture. Next, concrete cubes could be placed inside, squeezing extra polymer out. This method was preferred to the direct placement of the mortar cube and subsequent filling of the mold with geopolymer because it produced a uniformly coated sample. Since prepared geopolymer was relatively viscous and became more so with time, it did not flow easily into the gaps between the mold walls and the sample, leaving voids in the process. This problem was somewhat alleviated if the molds were vibrated after being filled.

Once the mold was filled to the top, it was covered with plastic film and placed into the oven at 65°C. Samples covered with MK geopolymer were kept in the oven for one hour, while MKS covered mortar was heated for four hours. Upon the removal of the samples from the oven, side pins were removed in order to prevent their binding to the geopolymer. Since the samples were not cured completely at that stage, they were left in the molds for about two more hours at room temperature, at which point they were removed from the molds.

Coated mortar samples were heated in the high temperature oven to 450°C and 800°C for one hour. They were then air-cooled to room temperature. After the completion of the heat treatment process the coating was removed. This was done in order to provide uniform testing area for each sample.

4.4 Sample Characterization

4.4.1 Geopolymer

Thermogravimetric analysis (TGA) is a technique that measures weight changes in a sample as a function of time or temperature. The analysis takes place under controlled conditions, including the rate of heat input and surrounding conditions. It is routinely used to determine a material's thermal stability. In the case of this research, TGA was used to confirm the ability of both geopolymer compositions to withstand high temperatures that may arise during fires or other emergency situations in both commercial and residential

environments. Thermogravimetric analysis was carried out at a heating rate of 10°C/min under oxygen flow using TA Instruments 2050 Thermogravimetric Analyzer in the Chemistry Department at Rochester Institute of Technology. 10 mg samples of the above-mentioned geopolymers were heated to 1000°C, the instrument's temperature limit, and held at this temperature for 10 min after reaching equilibrium.

Fourier transform infrared (FTIR) analysis was used to confirm the presence of polymeric material as described in the literature. FTIR is a technique that allows an identification of molecular structures within organic and polymeric materials based on the absorption of infrared light of various wavelengths. The absorption bands are characteristic of the material structure. Their intensities and shapes vary largely for different materials. IR spectra can be compared to the existing database to determine the nature of the structure at hand. Chemical concentration can be established by finding the area under the IR curve. It can then be compared to samples with known concentrations.

Infrared analysis of geopolymers was performed using a Bio-Rad FTS 3000 spectrometer in 600 to 4000 cm^{-1} wavenumber range. All spectra were obtained with a sensitivity of 4 cm^{-1} at 64 scans per spectrum. Both MK and MKS samples were polished with sandpaper after the curing stage was completed in order to improve the quality of the IR spectra.

Scanning electron microscopy, SEM, is used to produce a high magnification and resolution images of a surface with minimal sample preparation. Geopolymer morphology and structure can be examined and compared across the samples in order to determine structural changes due to different reactants present in the polymer. SEM also reflects whether geopolymer constituents undergo complete dissolution during material synthesis. Quantitative analysis in terms of size, shape, and distribution of the matter can be performed. MK and MKS samples were observed after being sputtered with a layer of gold. Characterization involved geopolymer exposed to 450°C and 800°C as well as the unheated samples.

4.4.2 Concrete

To confirm deterioration of concrete under elevated temperature conditions, mortar samples were subjected to thermogravimetric analysis. Settings identical to those for geopolymer characterization were used to perform the test.

Fourier Transform Infrared Analysis (FTIR) was carried out on five concrete samples using Research Series FTIR by UNICAM. One unheated specimen was used to establish a reference baseline for comparison purposes. To prepare the samples for FTIR study, concrete was crushed to powder and sifted with 180 μ m grid. Approximately 1mg of powder was then mixed with 200mg of KBr. The resulting mixture was compressed with five tons of pressure for five minutes using Grasbey Specac equipment, followed by ten minutes of compression at the pressure level of ten tons. The obtained sample was then used to perform infrared analysis. Obtained peaks were corrected by establishing a common baseline to facilitate further comparison.

Unlike geopolymeric material, concrete samples did not have to be coated with conductive material for use in the FEI Quanta 400 scanning electron microscope. Due to the nature of the equipment, low pressures could be used. This allowed for the observation of the material under conditions that are closer to the realistic environment. The size of the samples was chosen so that the photographs of the concrete's surface as well as its interior could be taken, permitting the comparison between the two.

Chapter 5

Analysis and Discussion

5.1 Geopolymer Characterization

5.1.1 Curing Behavior

After curing metakaolin-based polymer at 65°C for 90 minutes, it was observed that the resulting sample became hard. On the contrary, metakaolin-silica samples were still relatively soft after 4 hours of setting at the same temperature. This can be attributed to the ability of silica to absorb and retain water, which leads to a slower curing process. In addition, silicon to aluminum ratio in these samples was much higher than that in MK samples, influencing the curing behavior of the material. It was observed from the weight measurements presented in Table 5.1 that the weight after the curing was complete did not change significantly as compared to the original mass of the sample. This indicates that

| Sample | Percent Weight Loss, % | | |
|--------|------------------------|-------------------------|-------------------------|
| | After Curing at 65°C | After Exposure to 450°C | After Exposure to 800°C |
| MK | 1.5 | 32.5 | 33.3 |
| MKS | 1.7 | 35.8 | 35.3 |

Table 5.1: Weight loss of samples after curing and exposure to 450°C and 800°C

geopolymer tended to absorb water contained in the initial constituents, such as sodium hydroxide solution, and retained it until the evaporation temperature was reached. Since

the curing process was conducted at approximately 65°C and the sample was sealed with plastic film while in the oven, the water was not given off to the surrounding air.

In addition to the ability to retain water, it was also noticed that MK geopolymer was dimensionally stable. Such behavior supports the results obtained by Barbosa et al. [36] in their dilatometry study. On the other hand, MKS samples changed their shape with time if they were taken out of the mold immediately after being removed from the oven chamber. This means that geopolymerization was still in process and more than four hours are needed to achieve complete curing of the specimens. The observed dimensional changes are in agreement with conclusions reached by Donaldson et al. [32] that the polymerization reaction continues until the material is fully cured.

Some microcracking was observed on the surface of the metakaolin-based geopolymer several hours after the curing process was complete. The same behavior was reported by Barbosa [40] in the study of potassium polysialate. Gaps widened and deepened further with time. In the case of the metakaolin-based samples with an addition of silica, there were no visible cracks. It is believed that this was due to the slight expansion of the geopolymer and subsequent filling of the gap after the sample was removed from the mold and fully cured as discussed previously.

5.1.2 Thermogravimetric Analysis

Two main weight loss regions for the metakaolin-based (MK) sample can be observed in Figure 5.1. The first one occurs at 53°C. It may be attributed to the weight loss associated with water on or close to the surface of the polymer. The mass decrease up to approximately 100°C, corresponding to the evaporation of liquid that migrated to the surface during the heating process. Another slight peak in the weight loss is seen at 121°C. The sample continued losing weight up to 600°C, at which point its mass remained constant at 79% of the original value.

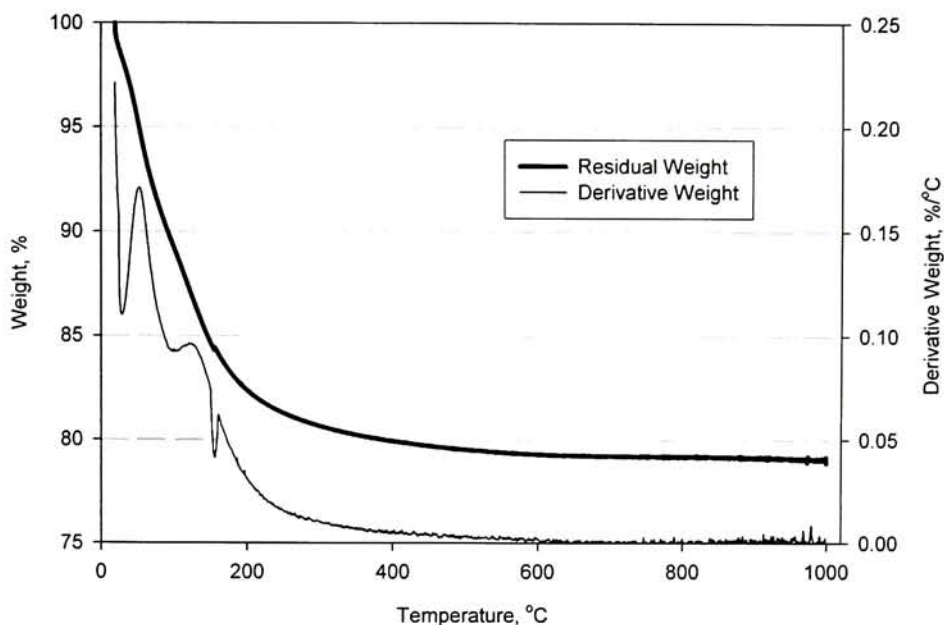


Figure 5.1: Thermogravimetric curves for metakaolin-based geopolymer at a heating rate of 10°C/min in oxygen atmosphere

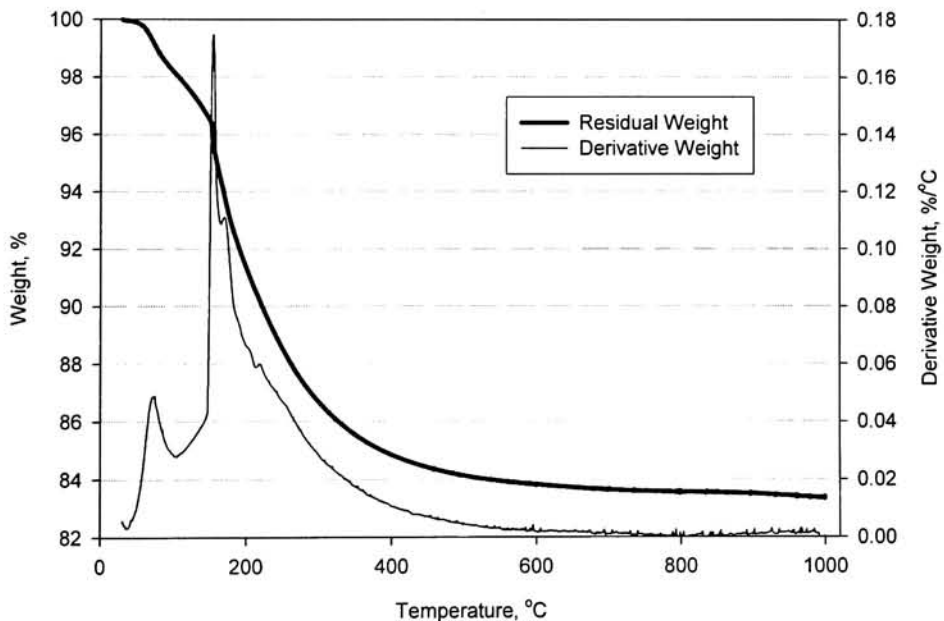


Figure 5.2: Thermogravimetric curves for metakaolin based material with addition of amorphous silica at a heating rate of 10°C/min in oxygen atmosphere

Figure 5.2 shows the residual weight and its derivative as a function of temperature for metakaolin-based geopolymer with amorphous silica. Its first mass loss near 75°C may be attributed to the initial evaporation of water from the material surface. The weight loss continued until approximately 550°C, peaking at 155°C. The mass remained constant thereafter at approximately 83% of the initial value.

Metakaolin/silica sample (MKS) followed the same basic trend as metakaolin material described above, but the main changes occurred at higher temperatures and samples retained larger portion of their initial weight as can be seen in Figure 5.2. While the largest decomposition of the MK sample was recorded at 53°C or less, silica-based polymer is characterized by much smaller initial weight loss and one large, well-defined peak at 155°C.

In addition, unlike MK geopolymer, MKS samples did not have any major secondary peaks on the derivative weight curve. A small increase was recorded at 72°C, but it is almost negligible in comparison to the main peak. Similarly to the MK sample, no additional weight loss was recorded at temperatures above 600°C, meaning that the material can be considered stable until the onset of 1000°C, the temperature limit of the instrument. One of the reasons that MKS sample exhibits greater stability as compared to the MK sample is that silicon-oxygen bonds with 368 kJ/mol bond enthalpy are among the strongest ones that silicon forms [44]. Molecules with strong chemical bonds has less tendency to undergo chemical change. Since MKS samples have higher percentage of these bonds due to the larger silica content, it retains its stability for a longer period of time. Overall, MKS polymer lost about 17% of its total weight during the heating process as indicated by the weight loss curve shown in Figure 5.2. This value is significantly different from that reported in Table 5.1 due to the sample size differences. The estimations listed in Table 5.1 are for the samples whose initial weight before curing was in the range of 100g. This sample size is believed to better represent materials' ability to retain water than that used for thermogravimetric analysis. Such behavior can be attributed to large surface area of TGA samples as compared to their overall weight and volume. In addition, excess water was able to migrate to the surface of

the specimen during the time required for sample preparation before the sample could be tested, resulting in lower values.

5.1.3 High Temperature Effects

Inspection of cured geopolymers after they were subjected to temperatures of 450°C and 800°C revealed large amount of cracking in MK samples, as presented in Figure 5.3. The number of gaps increased significantly after the exposure of the sample to 800°C. It

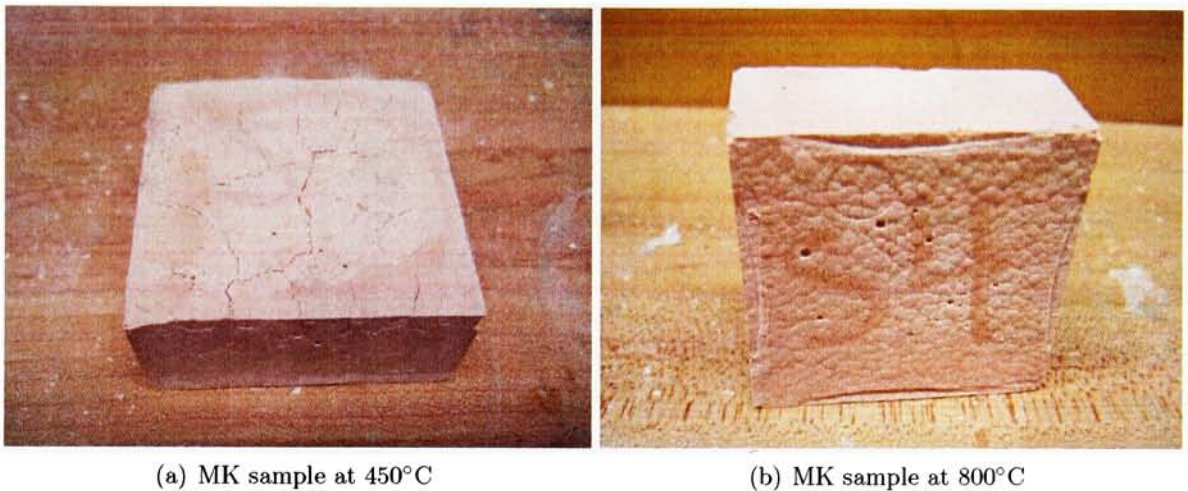
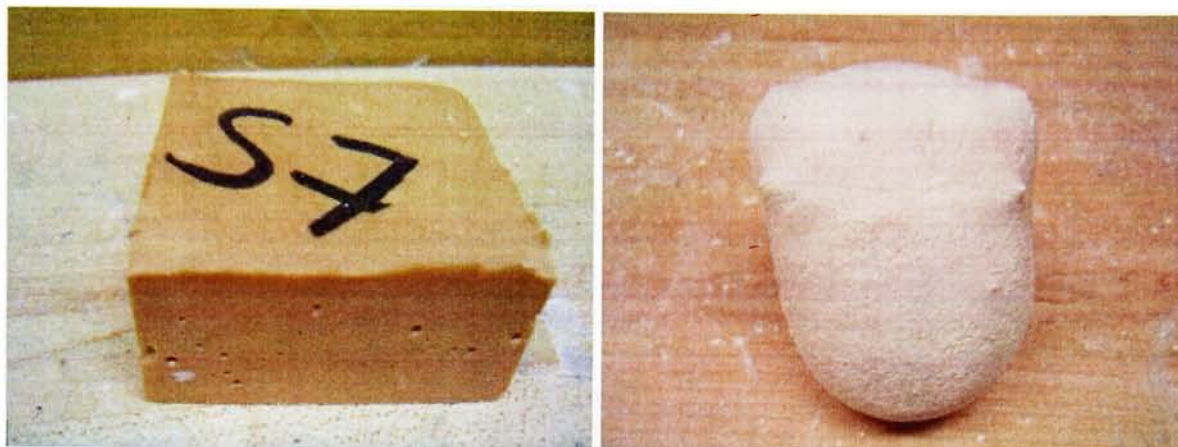


Figure 5.3: Cracking of metakaolin-based samples at 450°C and 800°C

is believed that gaps developed as trapped water migrated to the material surface through voids and air pockets. The formation of steam with volume many times that of liquid inside the sample during water evaporation resulted in the increase of gap widths. Geopolymer heated to 450°C maintained its structural stability while the one exposed to 800°C crumbled easily during handling.

MKS samples exhibited interesting behavior during the heating process. Unlike their metakaolin counterparts, samples containing amorphous silica did not retain their original shape and exhibited almost no cracking when exposed to 450°C. The foaming phenomena, characterized by the transformation of solid material into porous substance and accompanied by substantial volume changes, was observed immediately after the sample was placed into

the oven. Figure 5.4(b) shows significant amount of volume expansion when the sample is heated to 450°C. This behavior can be attributed to the transformation of large amounts of water trapped during the polymerization reaction into steam under high temperature conditions. According to chemical principles, gases occupy larger volumes than liquids,



(a) Room temperature

(b) 450°C



(c) 800°C

Figure 5.4: Metakaolin/silica sample expansion when subjected to elevated temperatures

resulting in uncontrolled expansion. Since the steam did not have pathways to migrate to the surface, it expanded inside the material, resulting in the overall volume increase.

The samples tended to shrink at much higher temperatures as illustrated in Figure 5.4(c). The resulting sample volume was much closer to the initial volume of the cured polymer. As the pressure inside each air pocket increased, the exerted internal force became greater

than the strength of the thin walls separating the steam from the outside air, resulting in the collapse of the material. This can be confirmed by the large amount of cracking and porosities seen on the sample fired at 800°C as compared to that exposed to 450°C.

Despite crack development at high temperatures, geopolymer samples did not disintegrate during the heating process and could be handled without crumbling when removed from high-temperature oven chamber. MKS specimen showed signs of delamination, forming a thin outside layer of material that separated the sample from the outside environment.

5.1.4 Fourier Transform Infrared Analysis

The IR spectrum of kaolin in Figure 5.5 corresponded well to that published in the literature [45][46]. It displayed a very strong and sharp peak at 1009-1032 cm^{-1} corresponding to Si-O bond stretching [28][47]. There is also a well-defined peak at 912 cm^{-1} associated with octahedral coordination of Al with OH. The presence of water in kaolin is confirmed by the broad pattern in the 3620-3694 cm^{-1} range.

Dehydroxilation of kaolin upon heating during its transformation to metakaolin is confirmed by the absence of peaks near 3600 cm^{-1} , as depicted in Figure 5.6. A peak at 1049 cm^{-1} corresponds to large concentration of Si-O bonds present in metakaolin. The shift of the peak to the right towards higher wavenumber during the heating process is characteristic of the conversion process. A peak at 797 cm^{-1} arises from Si-O-Al vibrations. Barbosa et al. [11] and Palomo et al. [28] reported observing a similar spectrum for metakaolin. The peaks could not be observed for wavenumbers less than 600 cm^{-1} due to the limitations of available equipment.

IR spectrum of the MK sample closely correlated with published information [11][29][38]. As shown in Figure 5.7, it exhibited a peak at 957 cm^{-1} corresponding to Si-O stretching vibrational bonds and asymmetric Al-O-Si stretching [38]. As compared to the metakaolin peak at 1049 cm^{-1} , this band has moved towards lower frequencies. This effect was previously observed in several other independent studies on geopolymer characterization [48].

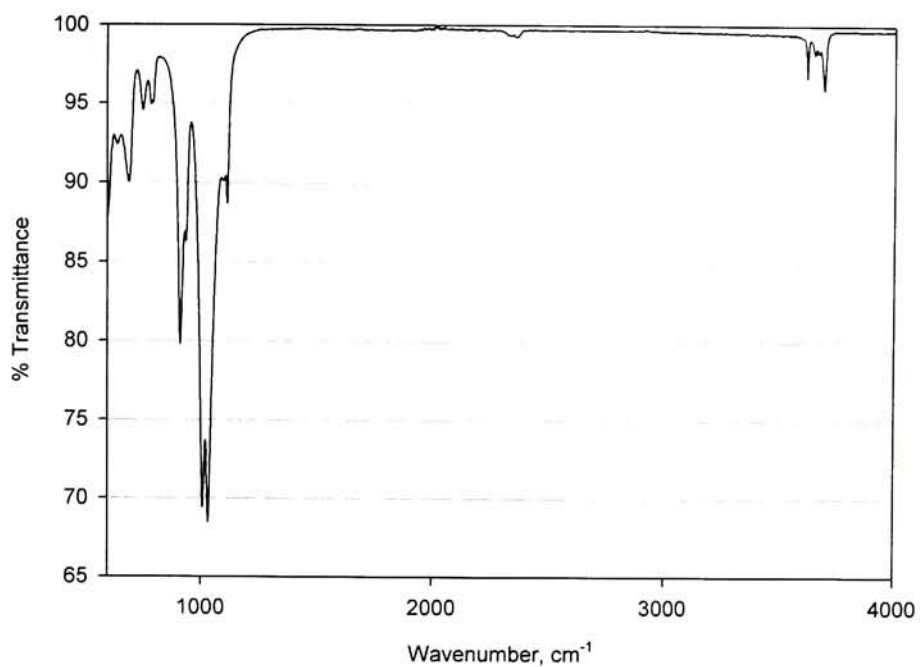


Figure 5.5: Infrared analysis of kaolin starting material

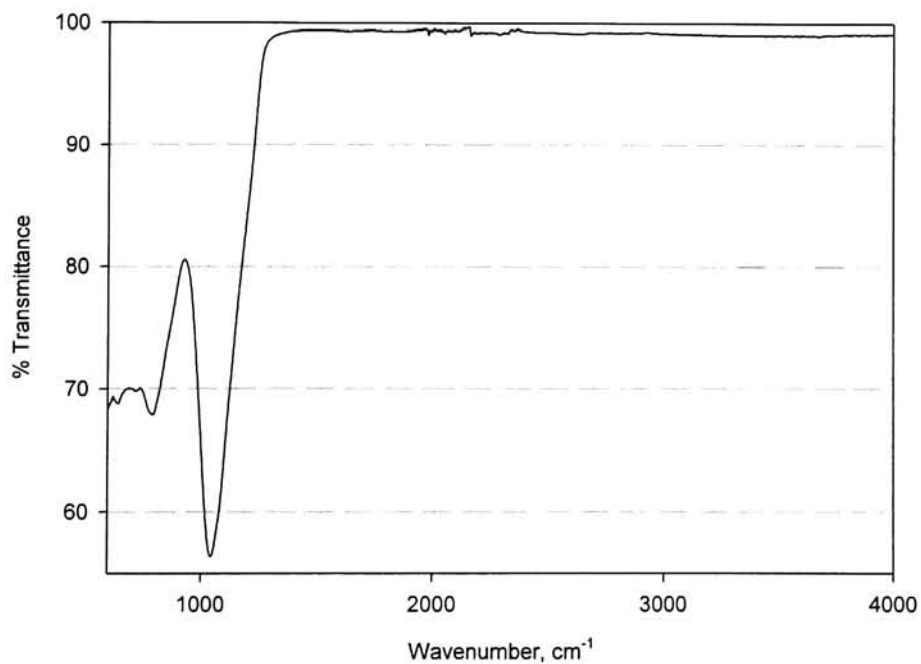


Figure 5.6: Infrared analysis of metakaolin

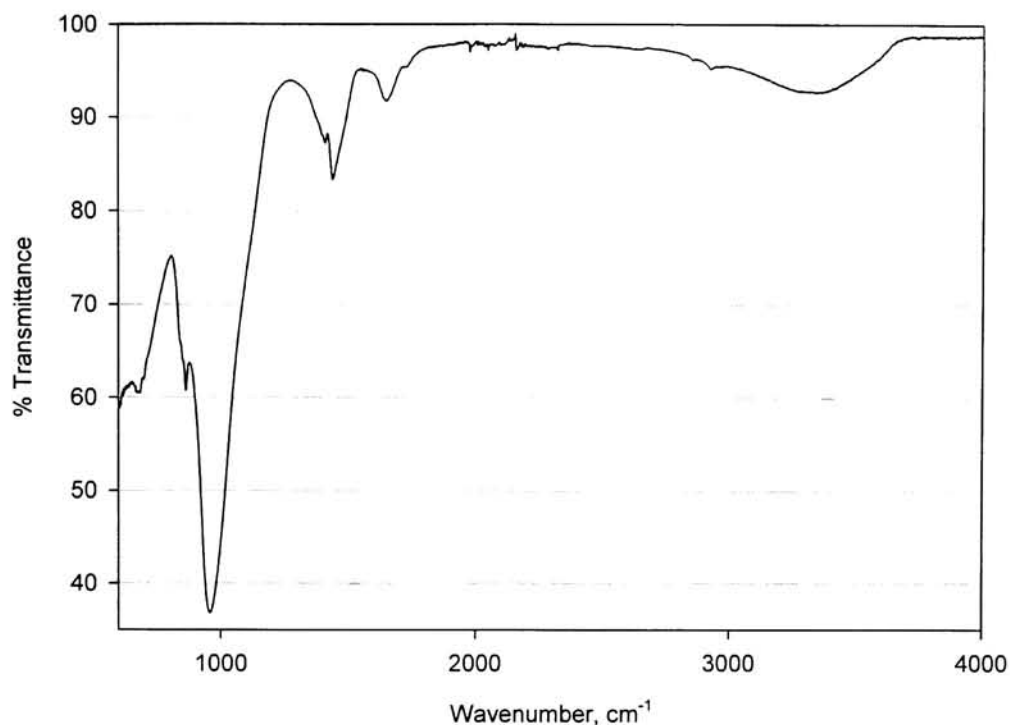


Figure 5.7: Infrared spectrum of metakaolin-based (MK) geopolymer

Two other medium intensity bands are observed at 1440 cm^{-1} with a 1410 cm^{-1} shoulder and 1648 cm^{-1} . One of the possible assignments of the first band may be to the stretching vibration of C-O bond that forms upon carbonation of sodium ions when they interact with the surrounding air, as reported by Barborsa et al. [11]. The presence of sodium carbonate may be confirmed by the correspondence of this peak to the characteristic feature of the Na_2CO_3 spectrum [49]. However, such assignment is not definite and other possibilities should be examined in the future. The second peak and the broad band in $3000\text{--}3600\text{ cm}^{-1}$ region indicate the presence of hydroxyl groups and absorbed atmospheric water, respectively. A close correspondence of all the peaks in the MK sample to those described in the literature confirms the claim that the material prepared for experimentation has similar characteristics with geopolymers used by other researchers.

The infrared spectrum of amorphous silica obtained from cat litter is shown in Figure 5.8. It shows a very strong peak at 1065 cm^{-1} and a medium peak at 799 cm^{-1} . These bands

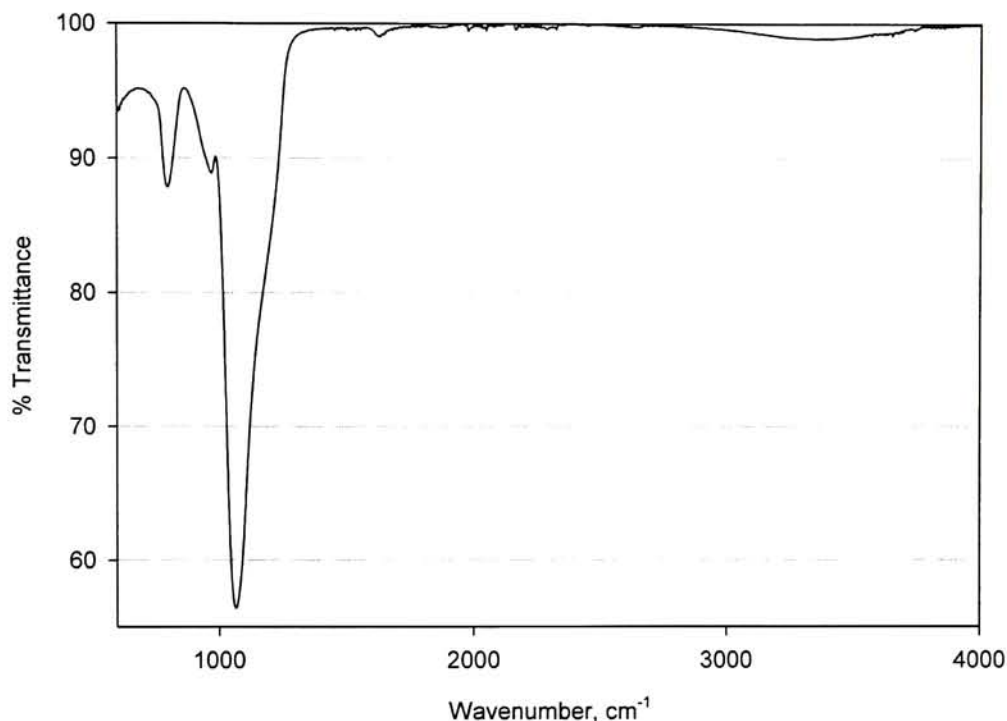


Figure 5.8: Infrared spectrum of silica

can be attributed to Si-O-Si asymmetric and symmetric stretches, respectively. A silanol bond (Si-OH) shown schematically in Figure 5.9 forms when the silica surface is exposed to the atmosphere. Peak at 972 cm^{-1} is due to the silanol Si-O stretch [27]. The material used in the experiments exhibits only a small peak corresponding to water due to the heating at 400°C as was described in the *Sample Preparation* section of this work. All other peaks correspond to silica's infrared frequencies, as outlined in published works [27][45]. It can be concluded from FTIR analysis of cat litter powder that it is a suitable source of amorphous silica.

Polymerization of the MKS sample resulted in a shift of the 1049 cm^{-1} band on metakaolin spectrum that arises from the vibration of Si-O bond to 972 cm^{-1} as shown in Figure 5.10.

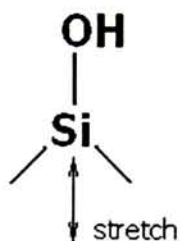


Figure 5.9: The structure of lone silanol

Once again, this peak is characteristic of the geopolymeric materials based on aluminum and silicon framework. This behavior is similar to that of the MK sample as described above.

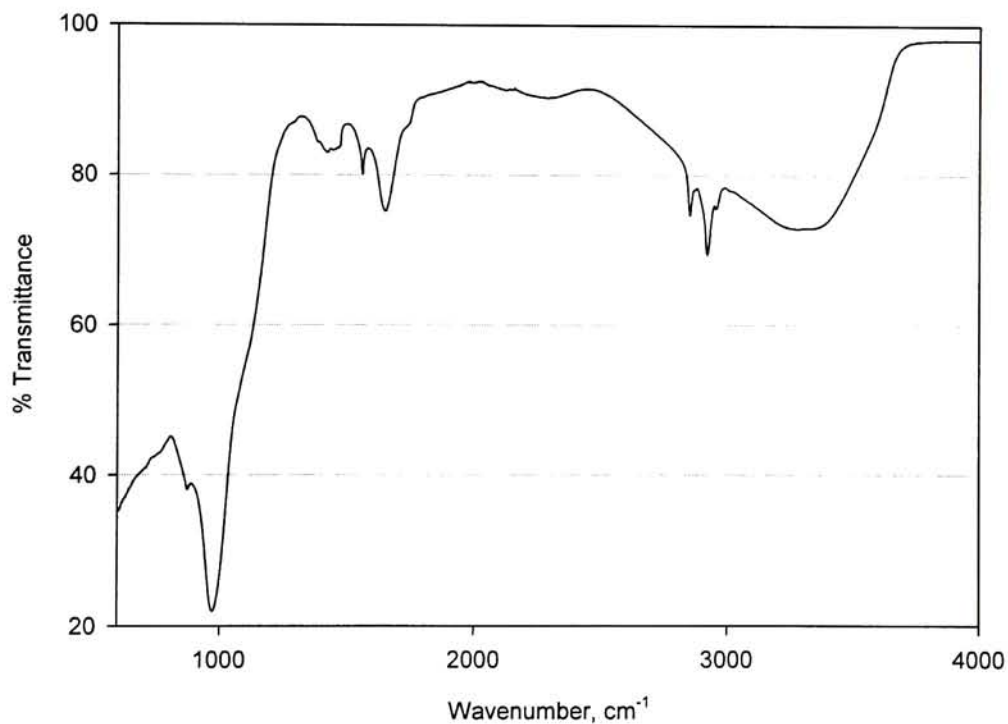


Figure 5.10: Infrared spectrum of metakaolin-based geopolymer with addition of amorphous silica (MKS)

The traces of carbonation were detected from the broad peak at 1418 cm^{-1} and a small sharp band near 1557 cm^{-1} . The presence of water in the geopolymer may be detected by

the development of the 1645 cm^{-1} peak and broad bands above 3200 cm^{-1} . A weak broad band developed around 2300 cm^{-1} . It is attributed to the presence of small amount of carbon dioxide, which has a very strong and sharp peak in this region [49].

5.1.5 Scanning Electron Microscopy

Figures 5.11 and 5.12 present micrographs of MK and MKS samples, respectively.

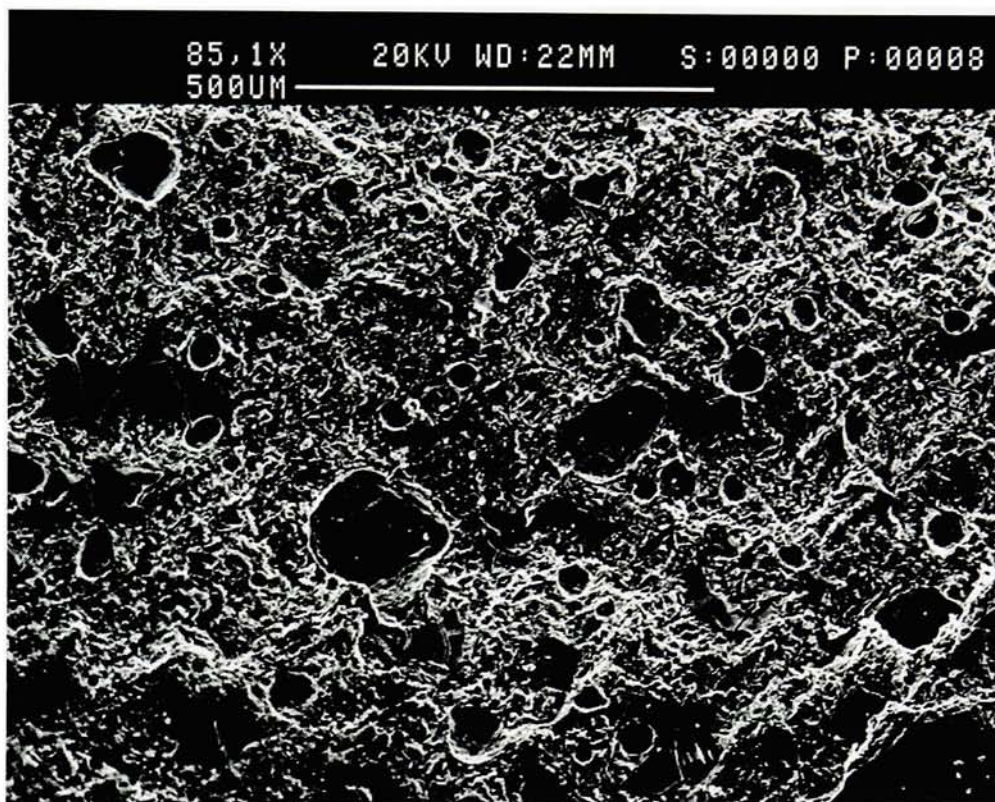


Figure 5.11: SEM micrograph of metakaolin-based geopolymer

Both geopolymers show high level of porosity visible even at low magnification levels. The metakaolin-based sample exhibited a rough surface with irregularly spaced voids. Pores greatly varied in size, reaching approximately $100\mu\text{m}$. Their presence could be attributed to the migration of trapped air or water within the material during polymerization and curing. As droplets moved to the surface of the geopolymer, they left behind unfilled pockets. Sample

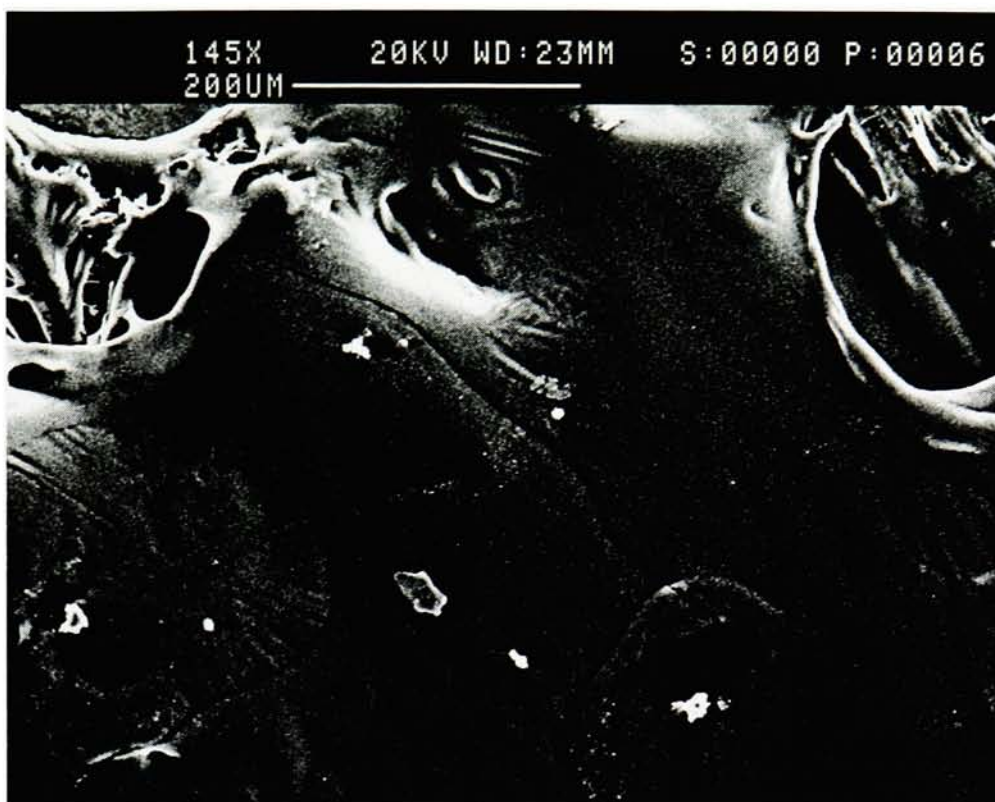


Figure 5.12: SEM micrograph of metakaolin-based geopolymer with addition of silica

preparation technique may have caused microporosity in the final solid. Additional vibration of samples after their pouring and the use of vacuum may decrease the number of trapped air bubbles present. However, Kriven et al. reported seeing the same phenomenon regardless of the method used [23]. The total number and pore size decreased, but it was impossible or impractical to eliminate all air pockets completely.

The MKS geopolymer exhibited a glassy surface with unevenly spaced dust particles of various sizes. This configuration is indicative of a material with amorphous structure. As compared to metakaolin-based geopolymer, an addition of silica resulted in the formation of larger pores, as big as $200\mu\text{m}$. It is believed that they also originated from the air bubbles entrapped inside the solid. The absence of well-defined and distinguishable particles within the MKS sample indicated that amorphous silica dissolved to a large extent within geopolymeric mixture.

Micrographs of MK and MKS geopolymers show cracks that developed between the air pockets, as illustrated in Figures 5.12 and 5.13. They are attributed to the movement of water vapor inside the material as trapped gas migrates to the surface during the curing stage.

The average gap width developed in both materials was measured to be approximately $3\mu\text{m}$. Cracks initiated by splitting the sample during its preparation were ignored. Those cracks were easily distinguishable from the ones formed during geopolymer curing as they did not originate from the air pockets, but rather started at the surfaces and disappeared with increased material thickness.

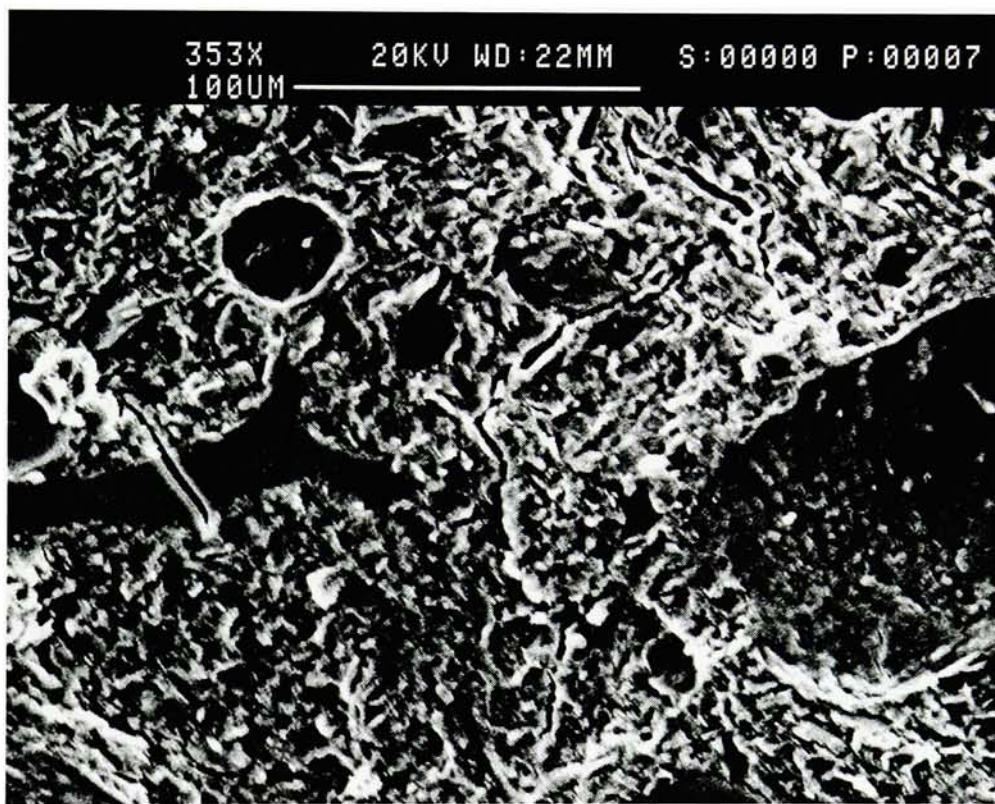


Figure 5.13: Cracking of metakaolin-based geopolymer at room temperature as revealed by SEM

Several micrographs of heat exposed samples were taken in addition to the ones described above in order to track any changes to microstructure. The MK sample almost does not exhibit any differences after being fired at 450°C for one hour. Observable cracks are wider

as illustrated in Figure 5.14, but there is approximately the same amount as in the unheated specimen. Grain size and shape also remained unchanged. This indicates that the material does not undergo significant changes upon heat treatment. It does not deteriorate due to the formation of new gaps. It is hypothesized that if the cured polymer did not have any cracks, only a small number of new ones would form in the high temperature environment. It is then possible to conclude that the cracking seen in Figure 5.3 is not due to the development of new cracks. Instead, geopolymer has microcracks present upon curing. They then propagate and widen further with increase in temperature.

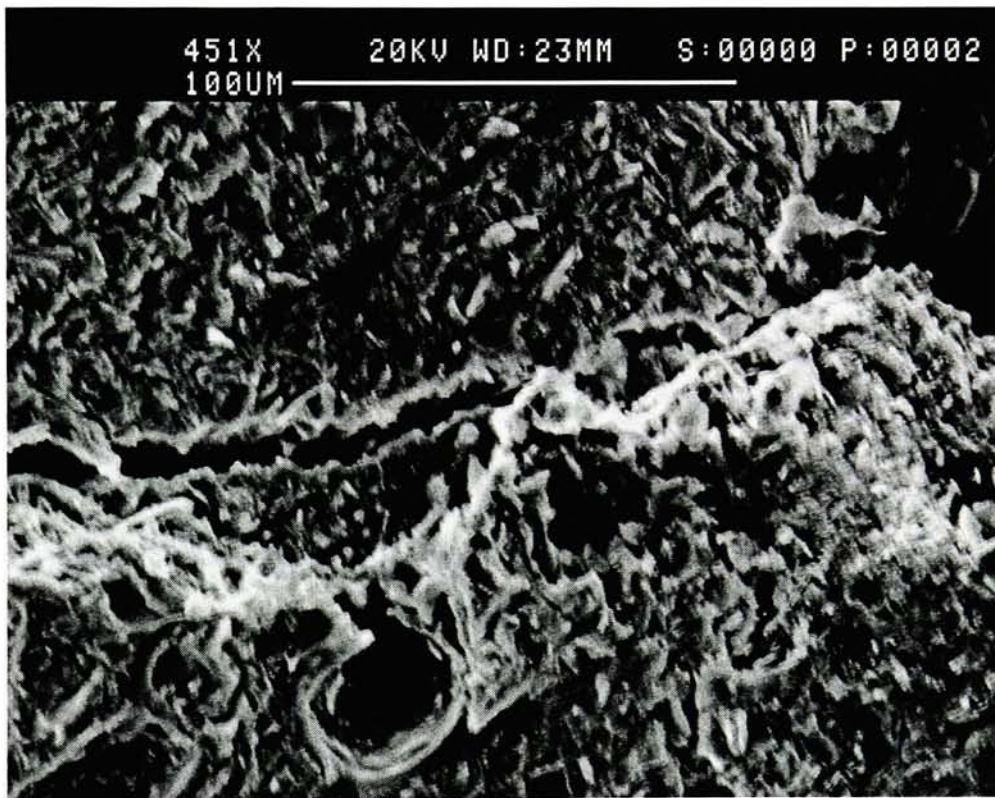
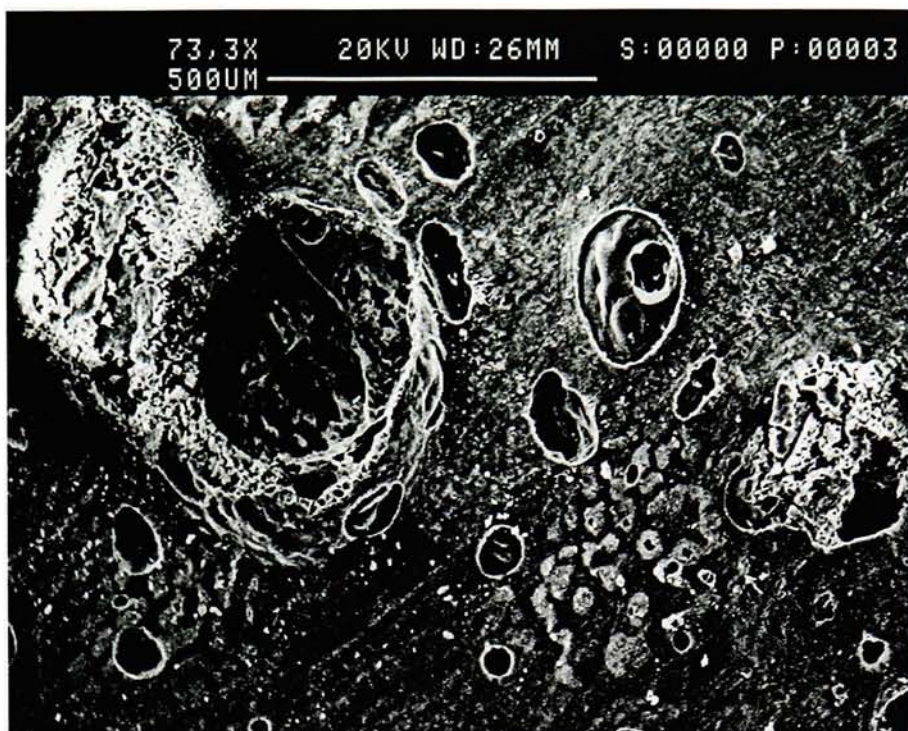
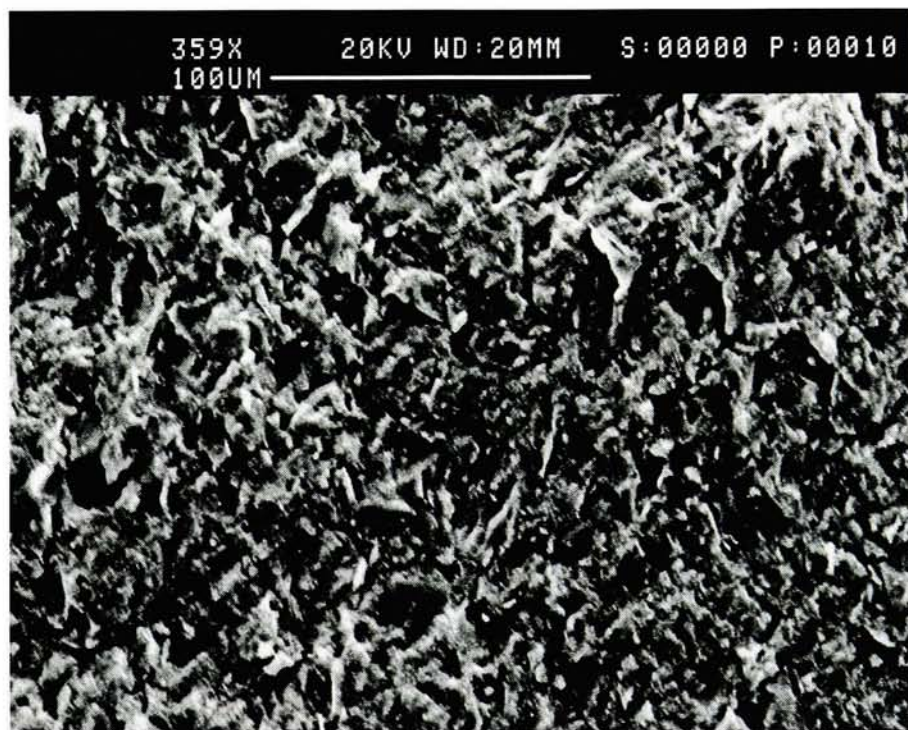


Figure 5.14: Cracking of metakaolin-based geopolymer at 450°C as revealed by SEM

More significant changes are seen in the MKS sample brought to 450°C and 800°C as shown in Figure 5.15(a). The surface was no longer smooth. Instead it was covered with a large number of small bumps that were visible even without a microscope. A micrograph taken at 73X (refer to Figure 5.15(a)) shows uneven rises, some of which contain holes.



(a) 450°C



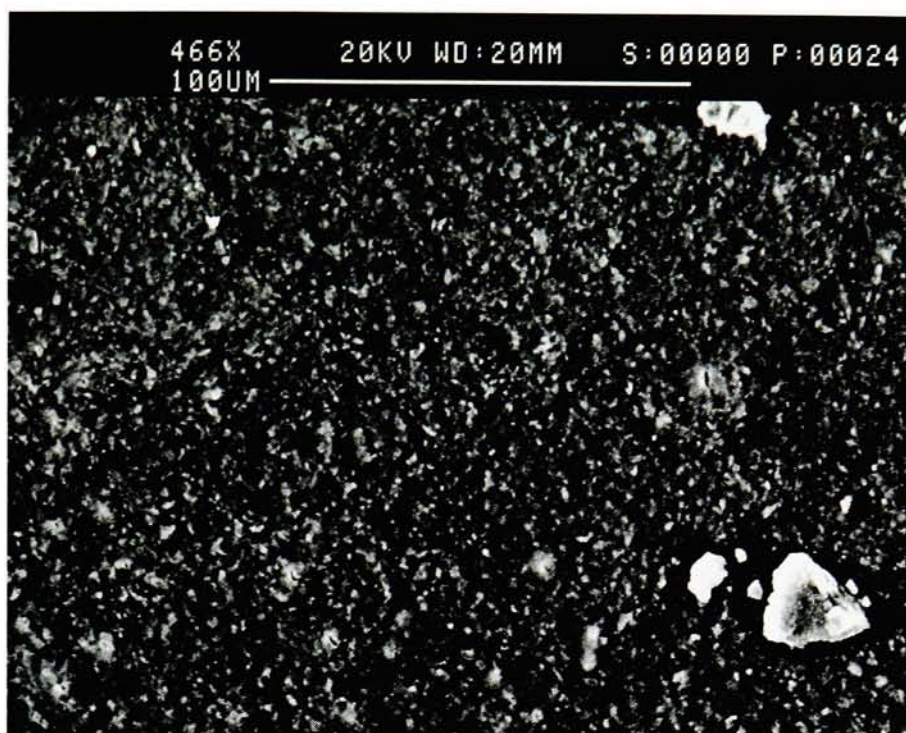
(b) 800°C

Figure 5.15: Surface of metakaolin-based geopolymer with addition of silica at 450°C and 800°C as revealed by SEM

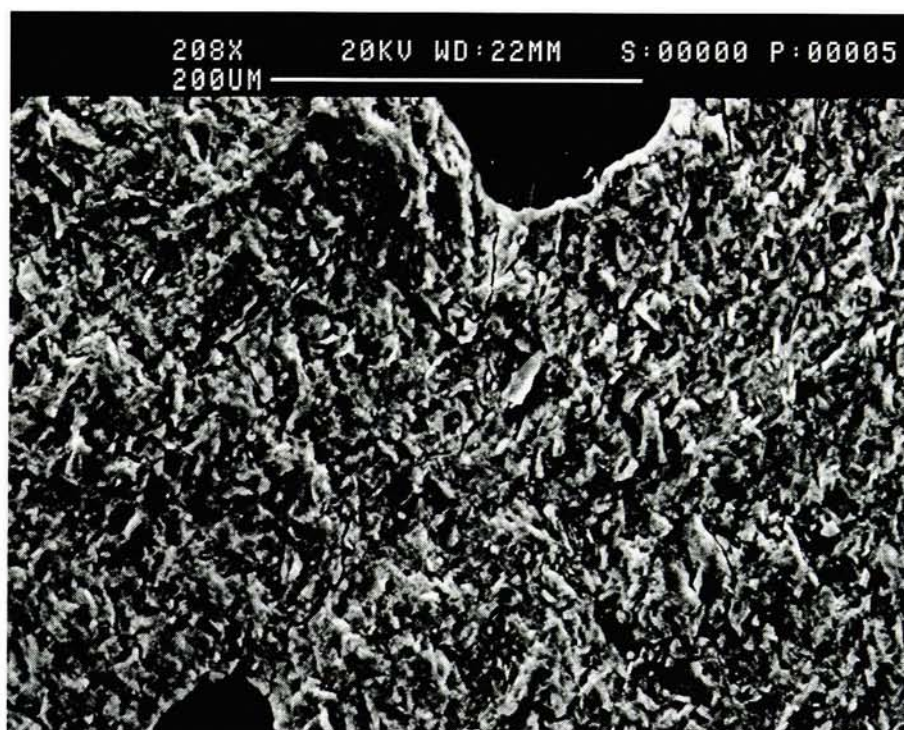
As described above, these elevated areas were formed during gas expansion. When the pressure force became greater than the strength of the material separating the gas from the outside environment, formed bubble collapsed, forming holes as big as $50\mu\text{m}$ wide.

The MKS samples further developed cracks at elevated temperatures. They were harder to distinguish due to surface changes, but could be seen relatively easily under higher magnifications as shown in Figure 5.16(a) on the next page. This phenomenon is even more pronounced in silica-containing samples fired at 800°C (Figure 5.16(b)).

Elevation variations on the surface of the MKS sample held at 800°C are more dramatic than in the specimen tested at 450°C . This is revealed by the color changes on SEM micrograph presented in Figure 5.15(b). Shades of grey correspond to the features located at different heights with respect to the observer with darker regions being further away.



(a) 450°C



(b) 800°C

Figure 5.16: Cracking of metakaolin-based geopolymer with addition of silica at 450°C and 800°C as revealed by SEM

5.2 Concrete

5.2.1 Thermogravimetric Analysis

Figure 5.17 shows thermogravimetric curves for an uncoated concrete sample. A moderate weight loss at 100°C can be observed, corresponding to water evaporation. The main decomposition of concrete, corresponding to the breakdown of CaCO_3 , begins around 455°C and reaches its maximum at 690°C [50]. This result confirms the claim in the literature that the main changes within concrete become noticeable at 400°C. It also supports the fact that concrete deteriorates at elevated temperatures and requires some form of protection.

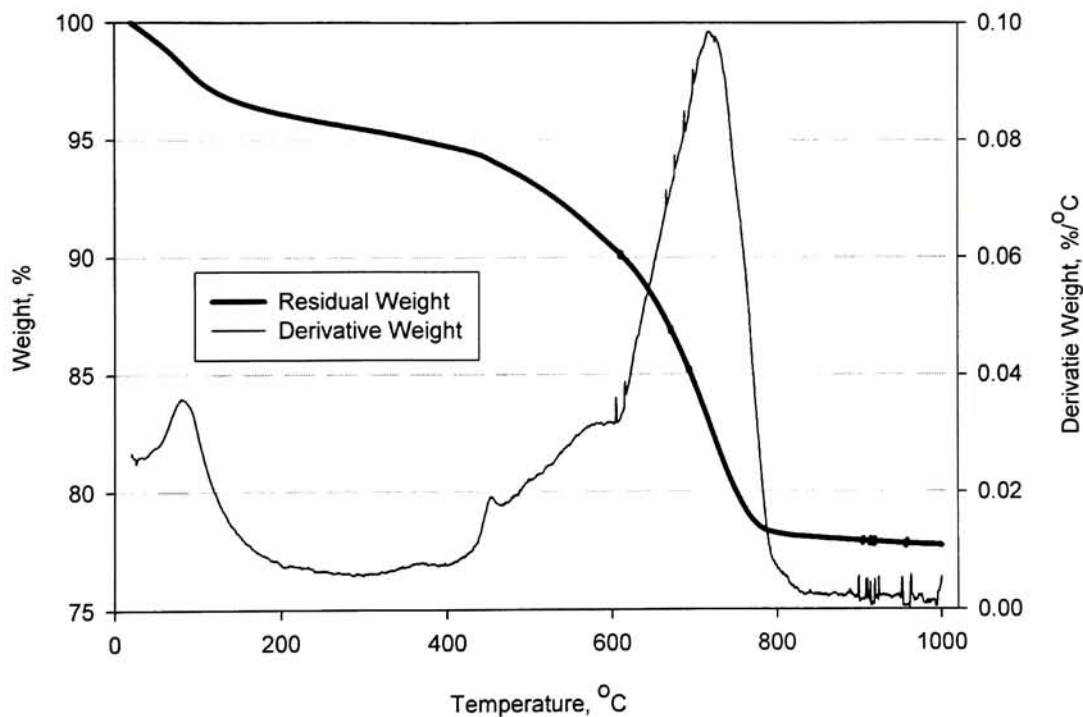


Figure 5.17: Thermogravimetric curves for mortar sample at a heating rate of 10°C/min in oxygen atmosphere

The comparison of thermogravimetric curves for geopolymer and mortar samples revealed that the geopolymer is stable in the regions where concrete starts undergoing chemical

changes. Both MK and MKS polymers exhibit only minimal weight loss at 400-600°C and derivative weight is approximately zero in the range of 600-1000°C, implying high resistance to thermal loading. It can be concluded based on the temperature response of the above-mentioned samples that geopolymer may be a suitable coating for the thermal protection of concrete.

5.2.2 Compressive Strength Measurements

In order to illustrate an application of geopolymer coatings to concrete structures, it is necessary to identify a performance measure, which can be compared across the samples heated to various degrees. The quality of concrete may be defined by the amount of load that can be applied before the structure undergoes yielding and subsequent collapse. Consequently, compressive strength was selected for comparison purposes. In addition, unlike some of the other mechanical and thermal properties, compressive strength can be easily measured with available equipment.

Mortar cubes were prepared in two distinct batches over the course of this research. However, since specimen composition, curing conditions, and testing methods were the same for both sets of samples, the compressive strength results were combined and presented as one group, unless otherwise noted. Measurements were taken at room temperature, 450°C, and 800°C. MTS Systems Corporation tensile/compression equipment was used to perform this testing.

A control group of mortars without any coating was selected to be tested under all of the above conditions. Compressive strengths obtained for coated cubes were later compared to the measurements of these unprotected samples as will be described shortly. The control group of mortar samples showed a well-pronounced negative relationship between the exposure temperature and the corresponding compressive strength. The data for the three temperatures are shown in Figure 5.18. This graph shows significant variation in the measurements taken at room temperature, which consequently, resulted in scattering of data

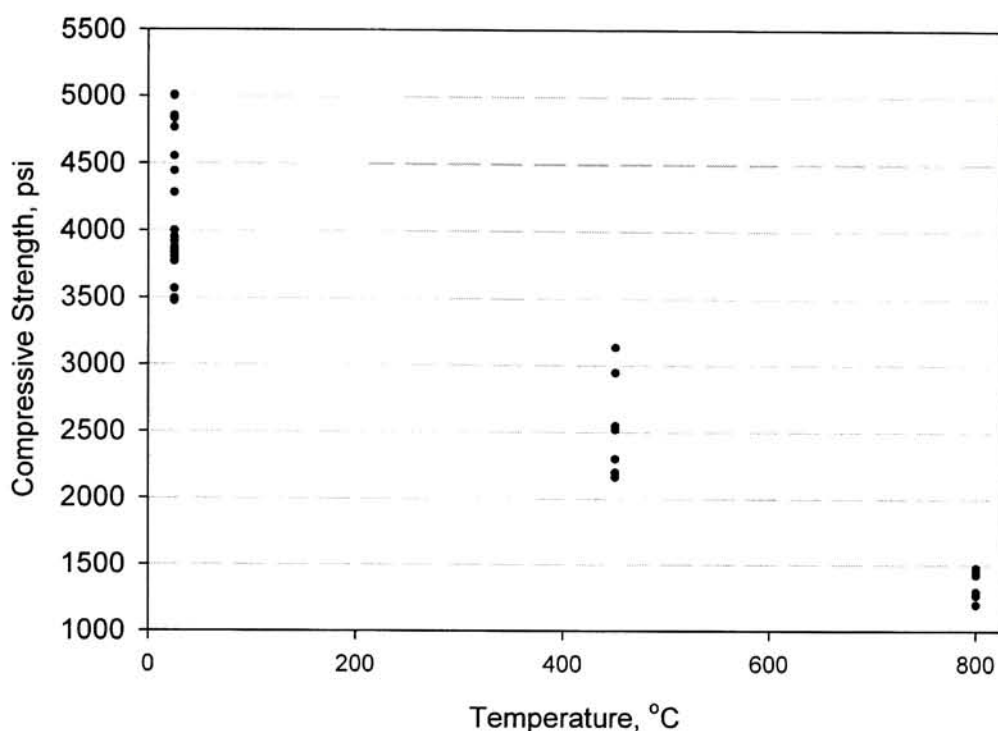


Figure 5.18: Compressive strength of unprotected mortar cubes (control group) in the range of 25-800°C

when samples were tested at higher temperatures. However, such behavior is not uncommon for experimental results. This work concentrated more on the observed trends rather than specific measurements. Several factors may be responsible for data variation. They include, but are not limited to the aggregate variability and the amount of force used to compact the mixture.

The graph revealed an apparent linear decrease in strength with rising temperature. However, many more experiments would have to be performed at other temperatures to confirm such a linear relationship. In general, an approximate decrease of 40% and more than 70% in the amount of compressive strength was recorded after the cubes were exposed to 450°C and 800°C, respectively. Such large losses are consistent with thermogravimetric analysis, which predicted the greatest decrease from 450°C to 700°C. At 30% of the remaining strength, the

structure will no longer be capable of carrying required loads, further emphasizing the need for thermal protection.

Coating mortar cubes with MK geopolymer significantly increased concrete's resistance to elevated temperatures. As illustrated in Figure 5.19, the compressive strength of the samples after heat exposure was lower than the initial values, but the downward drop was not as sharp. The compressive strength of the mortar was measured after the coating was

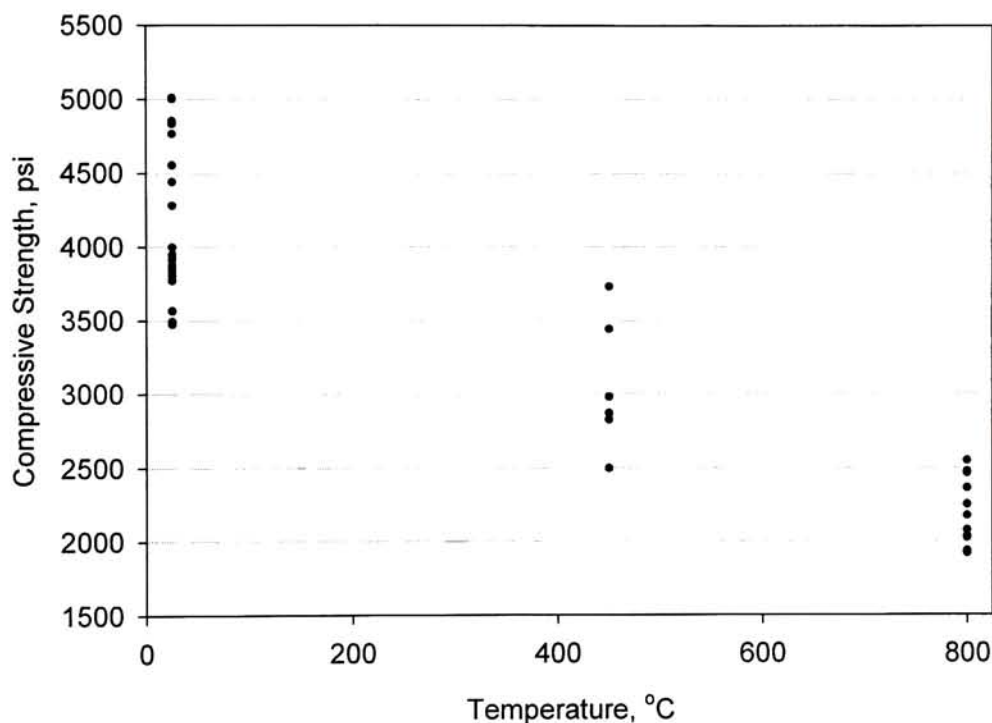


Figure 5.19: Compressive strength of mortar cubes coated with metakaolin-based geopolymer in the range of 25-800°C

removed. Consequently, the values obtained at room temperature would be the same for coated and control groups of cubes, allowing for the same data points to be used. Only one set of cubes was used in the analysis for this test group because unacceptably large variations were recorded for the other batch. On an average, the value recorded at 450°C for mortars

coated with metakaolin-based geopolymer is $12\pm 7\%$ higher than that seen for control group specimens. The difference went up to more than $20\pm 3\%$ at 800°C .

For the complete comparison, compressive strength measurements were taken after the exposure of silica-containing samples to 450°C and 800°C . The results are shown in Figure 5.20. The trend of strength loss for these groups of cubes was similar to that seen for

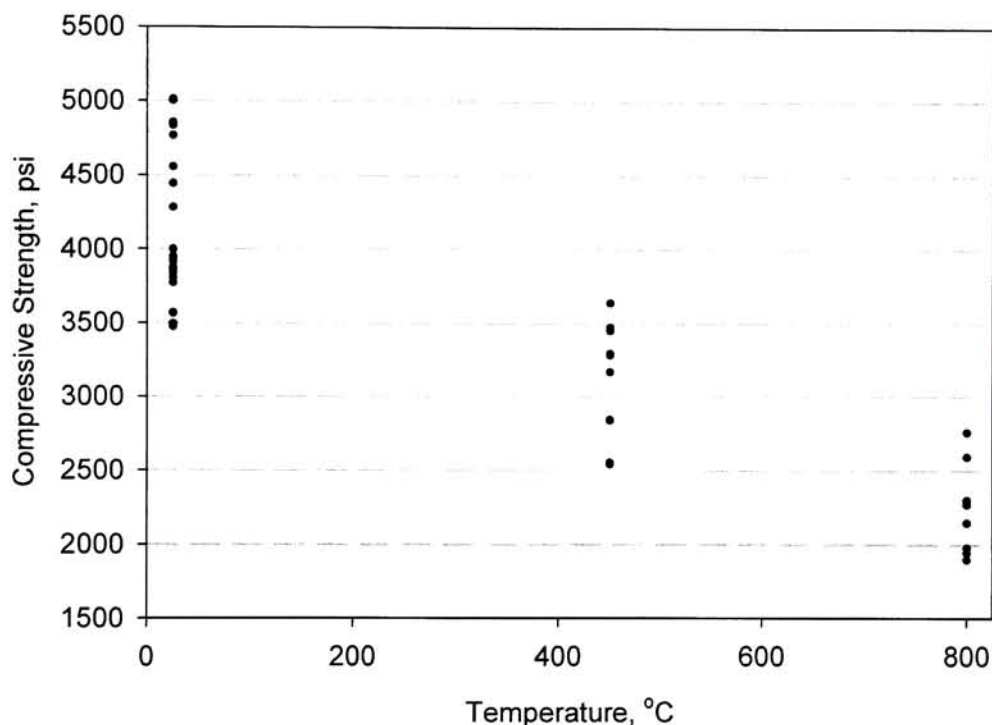


Figure 5.20: Compressive strength of mortar cubes coated with silica-containing metakaolin-based geopolymer in the range of $25\text{--}800^{\circ}\text{C}$

MK coated samples. The observed values were slightly higher in this case than for MK-covered samples. Even though the difference was not significant, it slowly increased with rising temperature. It is believed that the degree of thermal protection offered by MKS geopolymeric coating would be more pronounced at higher temperatures after a longer testing period.

In order to observe an overall trend of strength loss with temperature increase while concrete was being protected by each of the two geopolymer compositions, average values of compressive strength presented in Table 5.2 had to be calculated. They were then normalized

| Temperature °C | Percent of Original Strength, % | | |
|-------------------|---------------------------------|------------|-------------|
| | No Coating | MK Coating | MKS Coating |
| 25 | 100 | 100 | 100 |
| 450 | 61.6 | 73.7 | 75.3 |
| 800 | 32.5 | 53.4 | 54.2 |

Table 5.2: Percent original strength retained by the mortar after exposure to 450°C and 800°C

to 100% relative to the measurements taken at room temperature to create a trend graph in Figure 5.21.

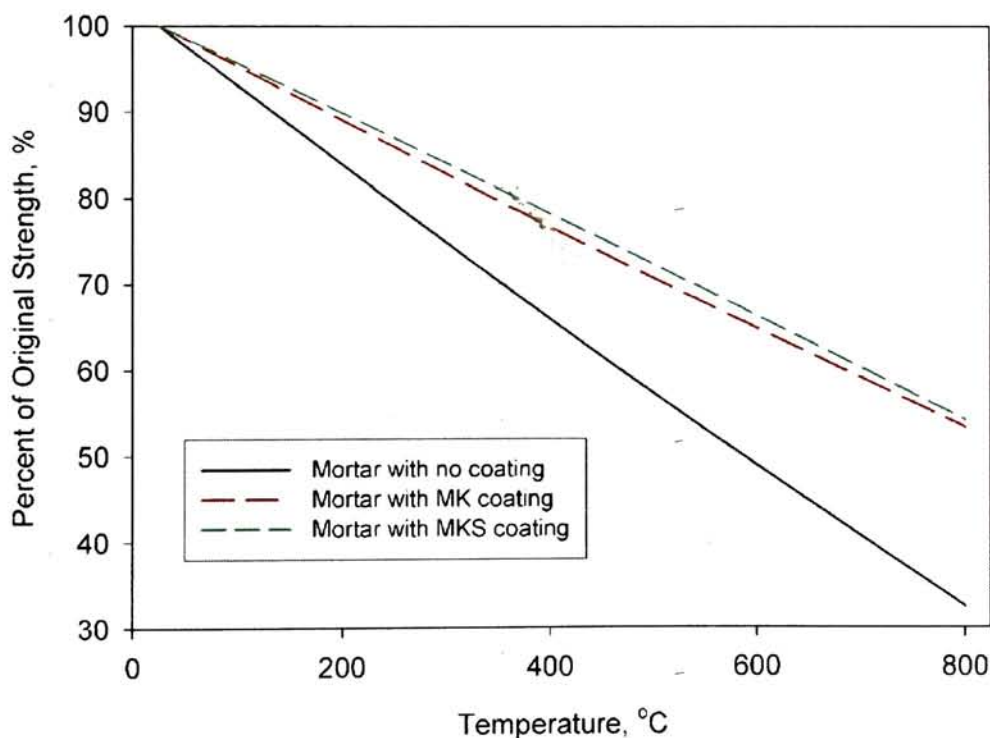


Figure 5.21: Trend of compressive strength loss over the 25-800°C temperature range for unprotected, MK-, and MKS-coated mortar cubes

From the graph, it can be seen that MK and MKS geopolymers offer comparable thermal protection to concrete. Almost 55% of the original strength is retained at 800°C as compared to the 32% without the coating. Amorphous silica-containing coating outperforms its counterpart at all of the tested temperatures. The differences between the two compositions diminished slightly with temperature increase. However, these differences may not be statistically significant due to the variation in the experimental data. Measurements taken at other temperatures would be helpful in establishing a more accurate trend of the strength loss.

5.2.3 Scanning Electron Microscopy

Concrete microstructure was compared across all samples in order to follow the changes on the microscopic level. The photographs, taken at the University of Trás-os-Montes and Alto Douro in Portugal, show signs of considerable deterioration with temperature.

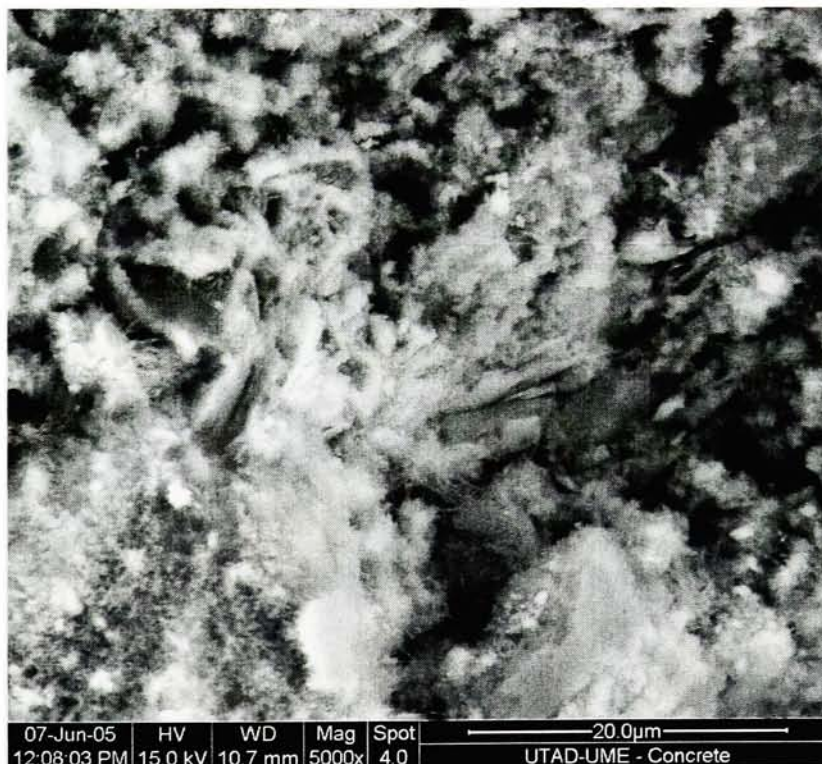


Figure 5.22: Micrograph of cured mortar

The microstructure of unprotected concrete shown in Figure 5.22 closely resembles that reported in the literature [51][52]. The matrix displays several hydrated phases, consisting primarily of calcium silicate hydrate (C-S-H), and smaller proportion of $\text{Ca}(\text{OH})_2$ (C-H) with visible aggregate particles and a few pores. Significant amount of damage can be easily detected at 450°C. It is characterized by the large amount of voids seen in Figure 5.23. The

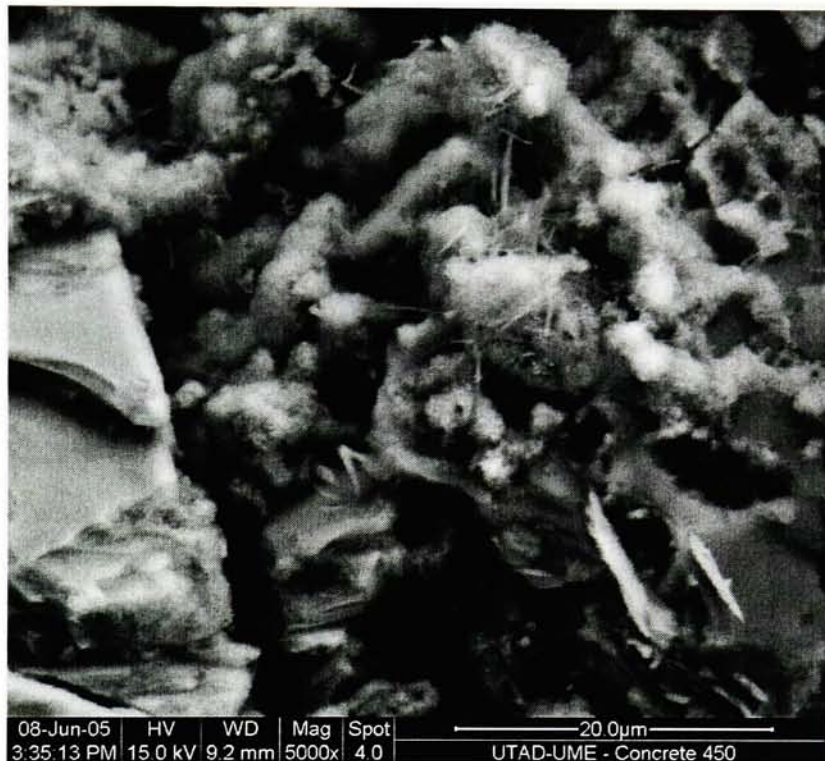


Figure 5.23: Mortar microstructure after exposure to 450°C

increase in void content could be the result of the loss of bound water. In addition, Figure 5.23 shows long cracks that developed alongside aggregate boundaries. Evaluation of the surface and interior parts of the mortar cubes revealed that the degree of thermal damage is significant in both locations.

Visible damage in the form of voids and deformation of $\text{Ca}(\text{OH})_2$ crystals is even more pronounced in samples exposed to 800°C as seen in Figure 5.24. As compared to the samples fired at 450°C, more microcracks could be observed within the material both on its surface

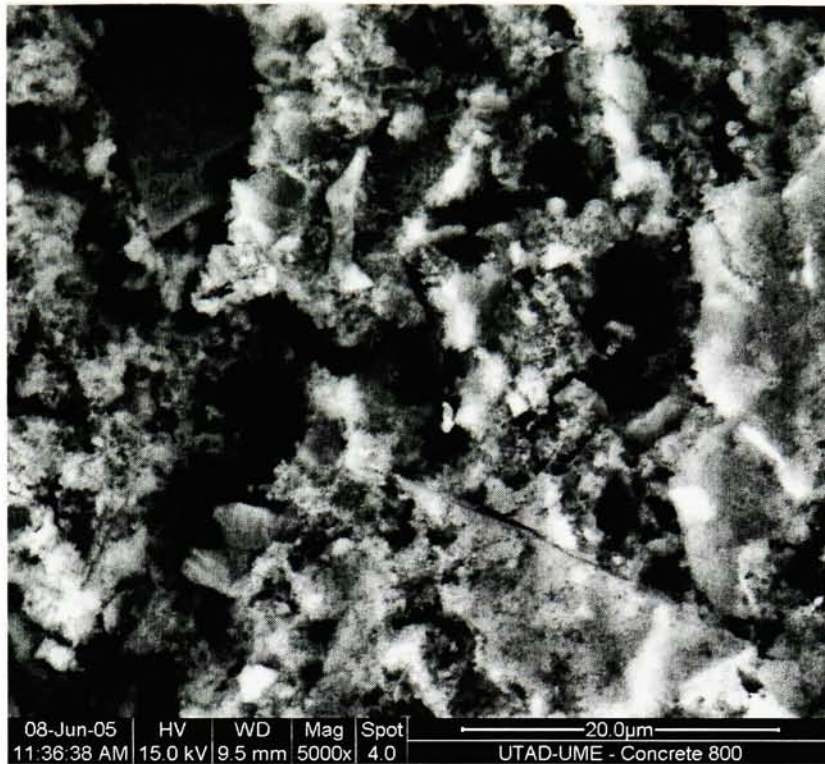
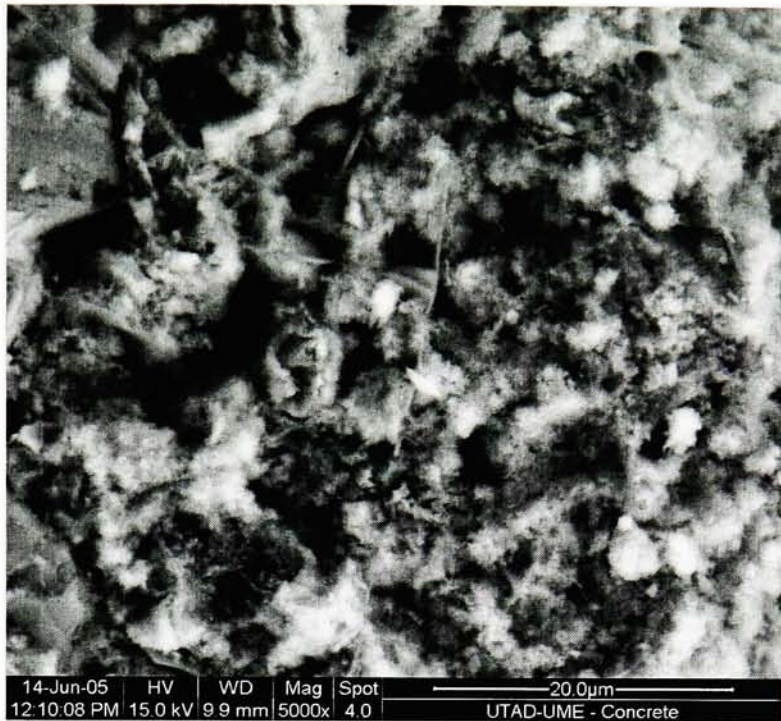


Figure 5.24: Mortar microstructure after exposure to 800°C

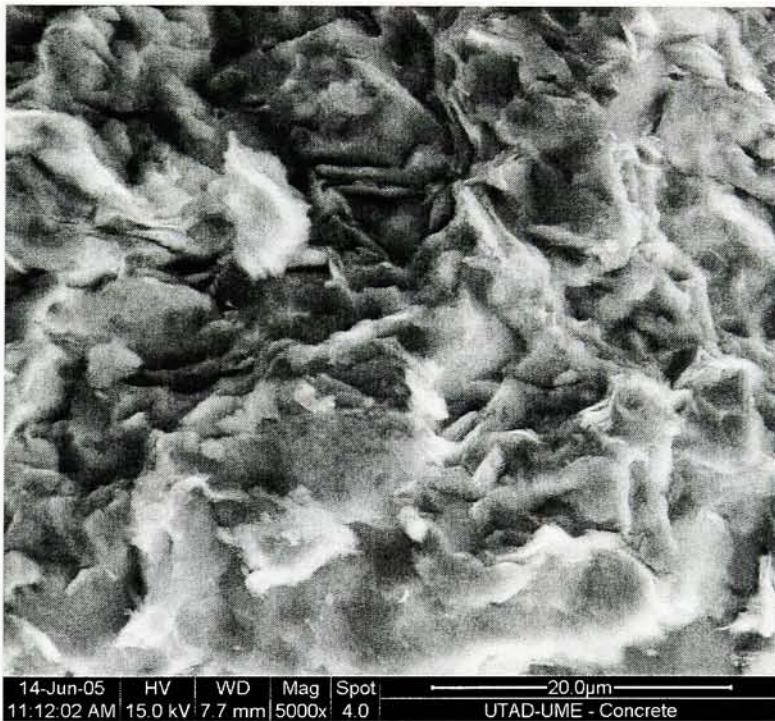
and in the interior part. Since the observed strength is directly related to the retention of moisture, the void content was a good indication of the amount of retained strength. As porosity of concrete increased, the load-carrying capacity decreased, explaining the significant drop in compressive strength.

The trend of mortar deterioration is apparent for geopolymer coated cubes as well, but the degree of damage is not as great. The interior microstructure of MK-covered cubes, shown in Figure 5.25(a), was similar to that of the unprotected concrete at room temperature.

As compared to the control group at 450°C, the amount of voids formed after the loss of constituent water was much less and they were significantly smaller in size. The average size of the openings seen on the unprotected mortar is approximately twice as big as that found in the MK-coated samples. Less damage to the microstructure translated directly into higher compressive strengths.



(a) Interior



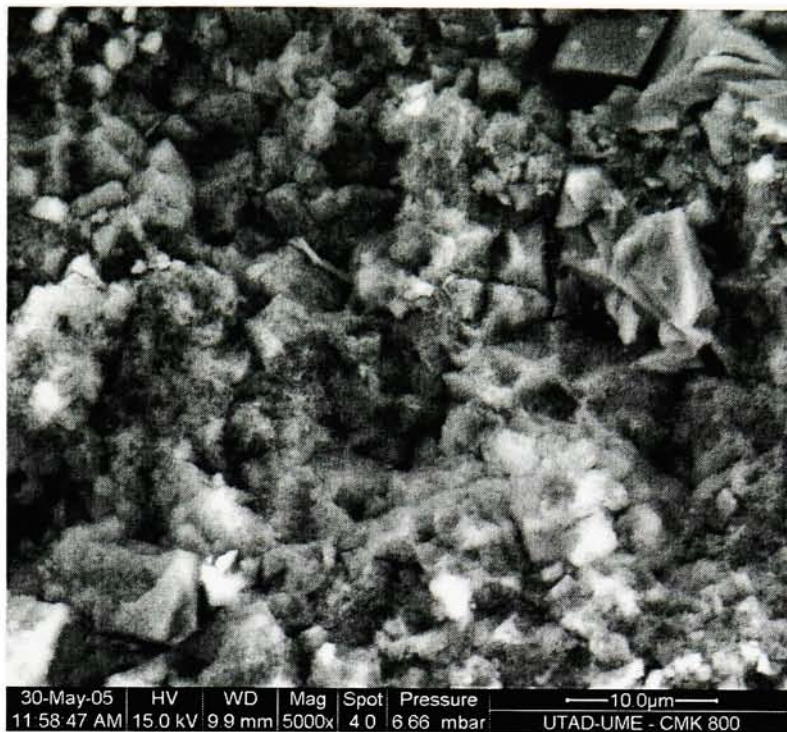
(b) Surface

Figure 5.25: MK-coated mortar microstructure after being exposed to 450°C

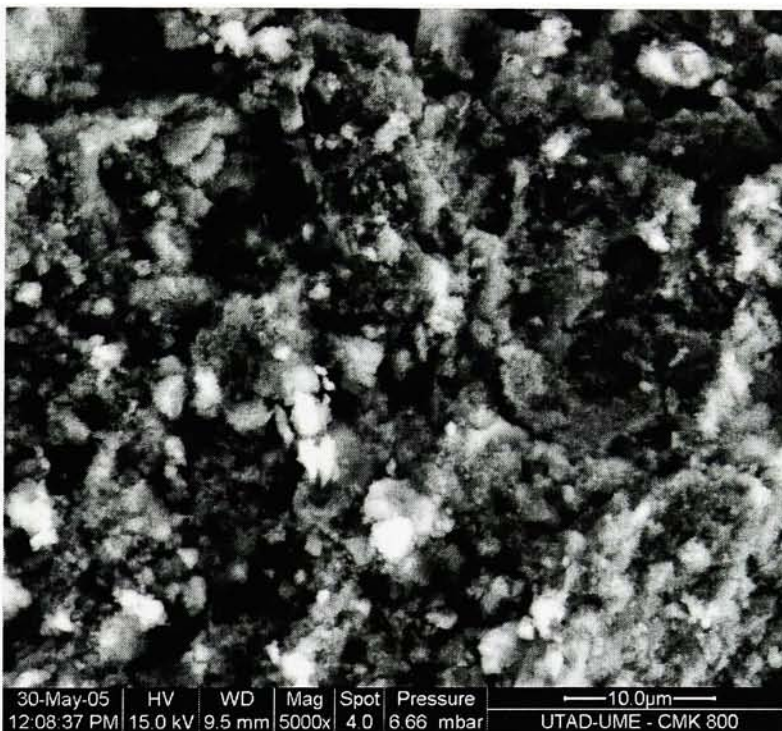
Unlike its interior part, an uncommon microstructure presented in Figure 5.25(b) was observed on the subsurface of the mortar specimen. The matrix appeared to be a lot more homogeneous and fused in a continuous pattern so that there were no visible pores. However, sintering should not have been detected after heat treatment at 450°C as this temperature is too low for the particle fusion to occur. It was thus hypothesized that a chemical reaction takes place on the mortar/geopolymer interface. Since concrete is rich in silicon and aluminum, it produced a favorable environment for the infiltration of constituent water present in geopolymer. The above-mentioned reaction takes place only on the concrete surface, extending no more than several millimeters deep judging from the micrographs of the sample taken at different locations.

As seen in Figure 5.26, at 800°C the microstructure was more open both on the surface and the interior, resembling the photograph of unprotected concrete taken at 450°C. The pattern of continuity was still observed on the surface. However, some aggregate particles and damaged concrete matrix were distinguished as well. The sample became more porous towards the interior part of the cube. The void content was much less than that seen in Figure 5.24, but the microstructure was comparable.

SEM photographs of MKS-coated mortar presented in Figure 5.27 exhibited more similarities with those for plain concrete rather than MK-protected cubes. The void content was significantly less than for the unprotected samples, but there were no visible signs of sintering both on the surface and in the interior of heat treated cubes. At 450°C and 800°C, only a few pores could be detected. Overall, both micrographs resembled the one in Figure 5.22 with the exception of crystal deformation seen at 800°C. Consequently, since the microstructure of the MKS-coated cube suffered minimal damages, its final compressive strength would be higher than that recorded for the unprotected concrete.

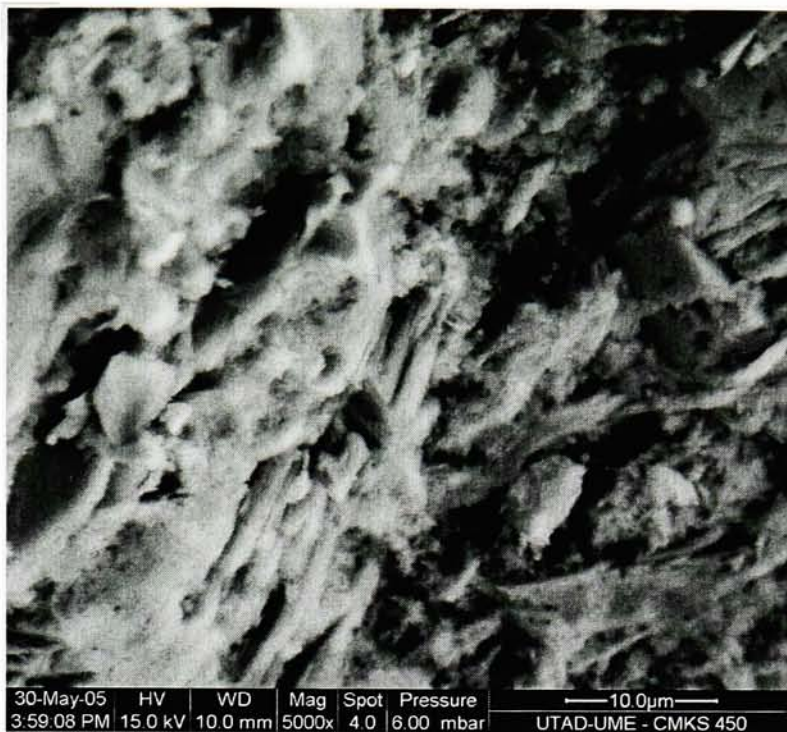


(a) Surface



(b) Interior

Figure 5.26: MK-coated mortar microstructure after being exposed to 800°C



(a) 450°C



(b) 800°C

Figure 5.27: MKS-coated mortar microstructure (interior) after being exposed to 450°C and 800°C

5.2.4 Fourier Transform Infrared Analysis

Fourier Transform Infrared analysis, performed during the visit to Portugal, revealed some definitive changes that occurred when concrete was exposed to various temperatures. The spectrum for the unheated mortar cube, presented in Figure 5.28, was taken as a reference for comparing the samples. It showed peaks characteristic of calcium carbonate bonds

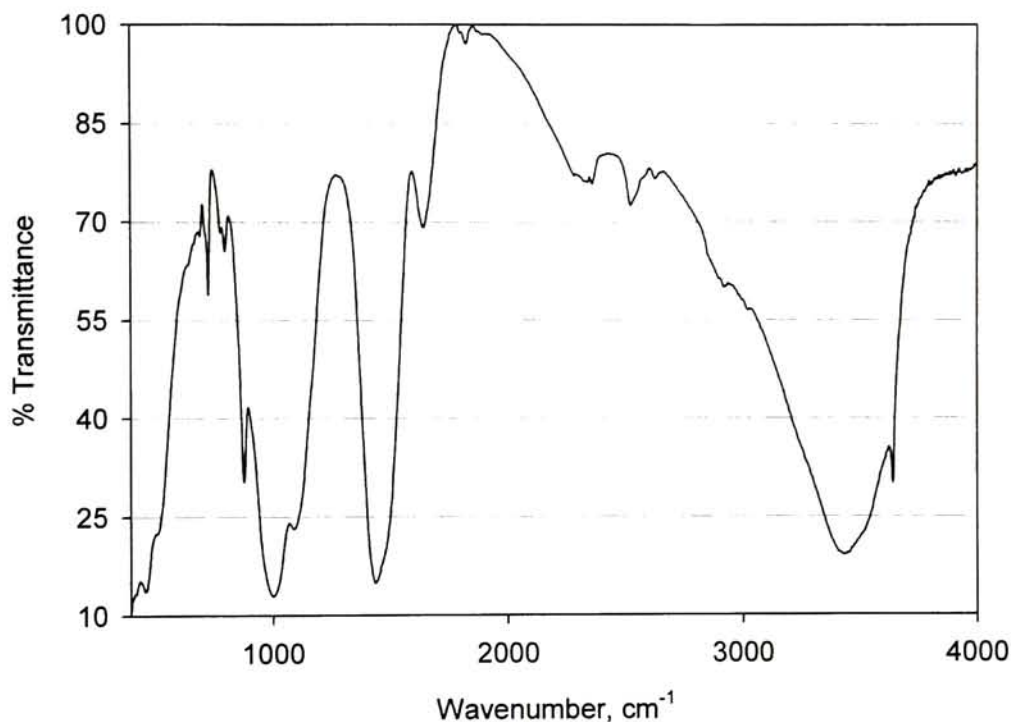


Figure 5.28: Infrared spectrum of unheated concrete

in concrete in the 1434 cm^{-1} and 877 cm^{-1} regions. They correspond to C-O stretching and C-O out-of-plane bending, respectively [27][45][50]. The band at 1000 cm^{-1} correspond to vibrational bonds in amorphous silica present in cement and sand as was described in the section on infrared analysis of geopolymers. Constituent water contained within the samples is indicated by the peaks at 3430 cm^{-1} and 1639 cm^{-1} .

Infrared spectra of heated cubes exhibited similar peaks as can be seen in Figures 5.29(a) and 5.29(b). Si-O band around 1000 cm^{-1} shifted towards slightly lower wavenumbers, while a shoulder associated with Al-OH group, visible on the spectrum taken at room temperature at 1087 cm^{-1} , separated from the main peak and developed into a well pronounced band at 1147 cm^{-1} . The loss of constituent water is visible through the shrinkage of the broad peak around 3430 cm^{-1} and 1640 cm^{-1} .

In the case of mortar samples protected with metakaolin-based coating, the changes are not very apparent, especially in the case of cubes exposed to 450°C as presented in Figure 5.30. The amount of water loss is significant comparing with the unprotected specimen fired at the same temperatures. However, the intensity of the peak in Figure 5.30(b) developed at 1147 cm^{-1} is not as great as that observed for the uncoated cubes. In addition, there is no shoulder in the 1500 cm^{-1} region that could be seen for unprotected concrete heat treated at 800°C .

As presented in Figure 5.31, infrared spectrums of MKS-coated mortars are similar to the MK-covered samples described above. At 450°C , the damage is minimal. It is characterized by the evaporation of water seen as the absorbance reduction at 3430 cm^{-1} and 1640 cm^{-1} . In addition, a small shift of the Si-O band at 995 cm^{-1} as well as the disappearance of the shoulder at 1087 cm^{-1} were observed for heated specimens coated with MKS geopolymer. In general, the changes presented in the IR spectrum of MKS-protected cubes are less pronounced at high temperatures than those seen for the metakaolin-based coating.

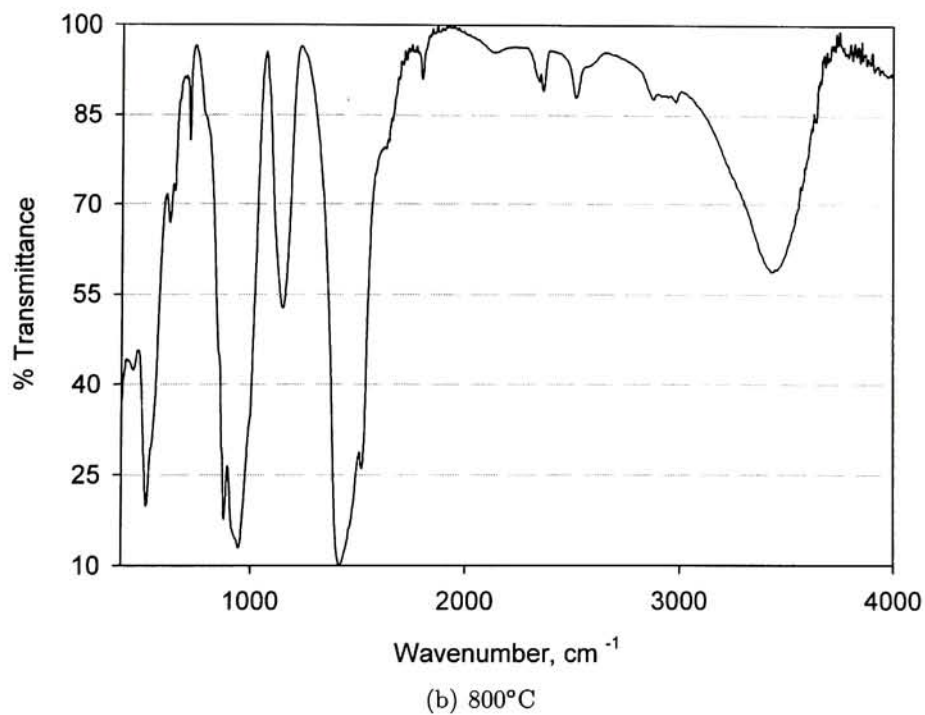
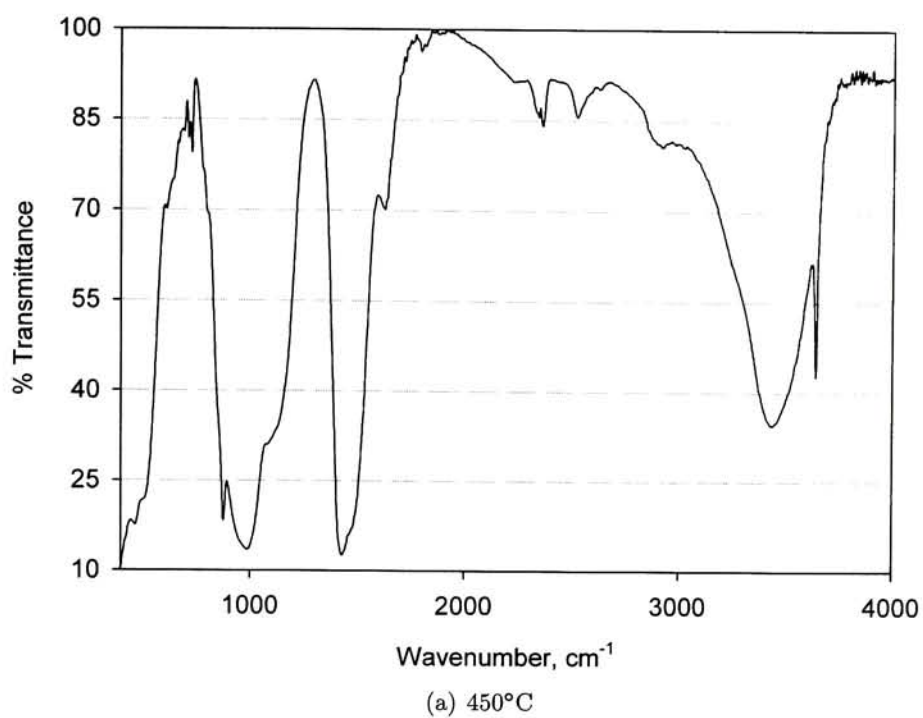


Figure 5.29: Infrared spectra of concrete exposed to 450°C and 800°C

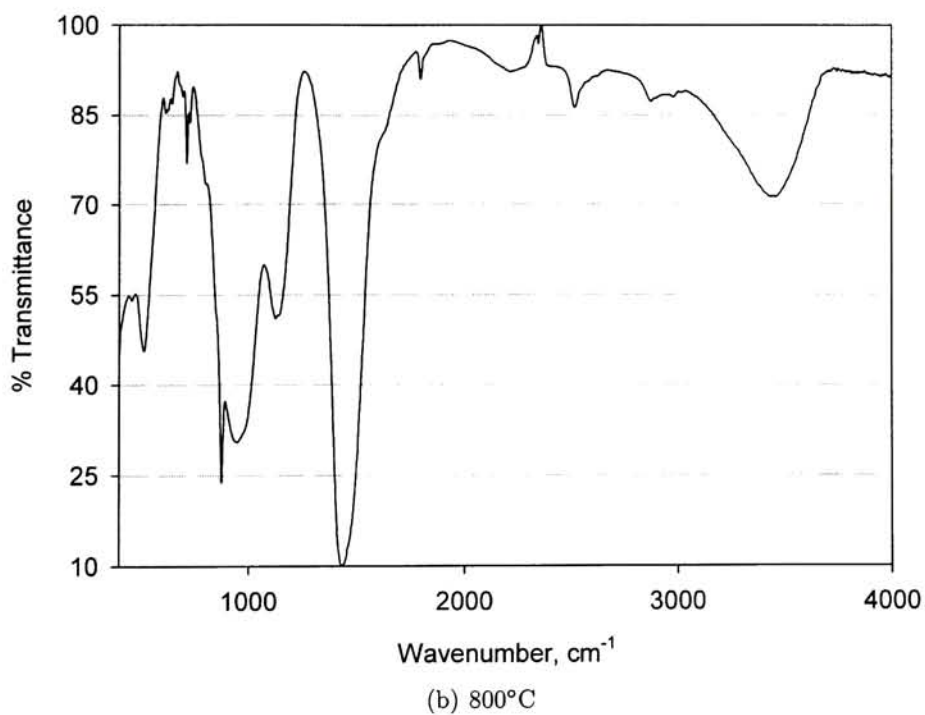
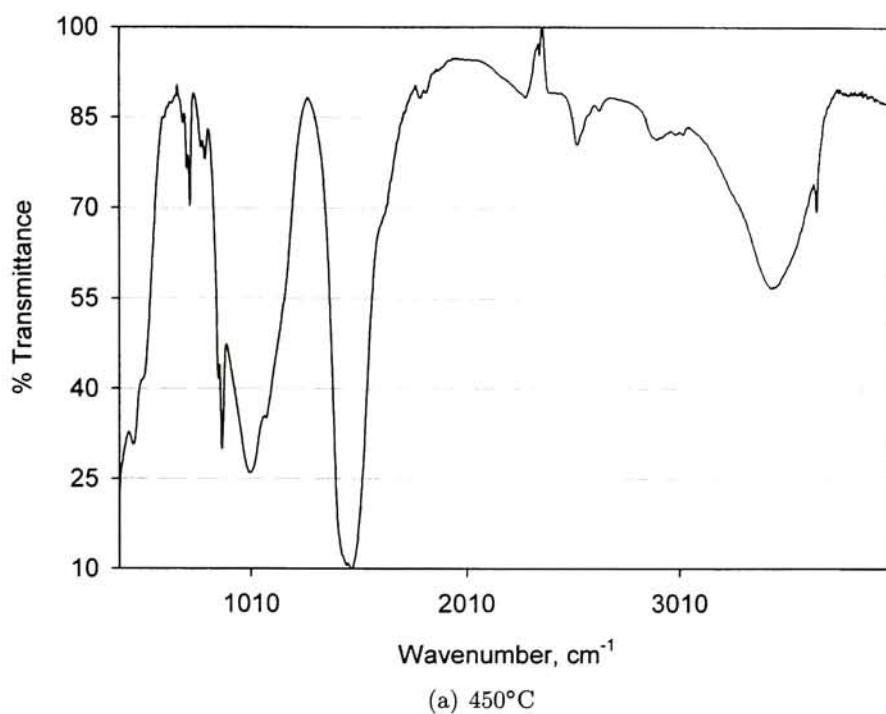


Figure 5.30: Infrared spectra of MK-coated concrete exposed to 450°C and 800°C

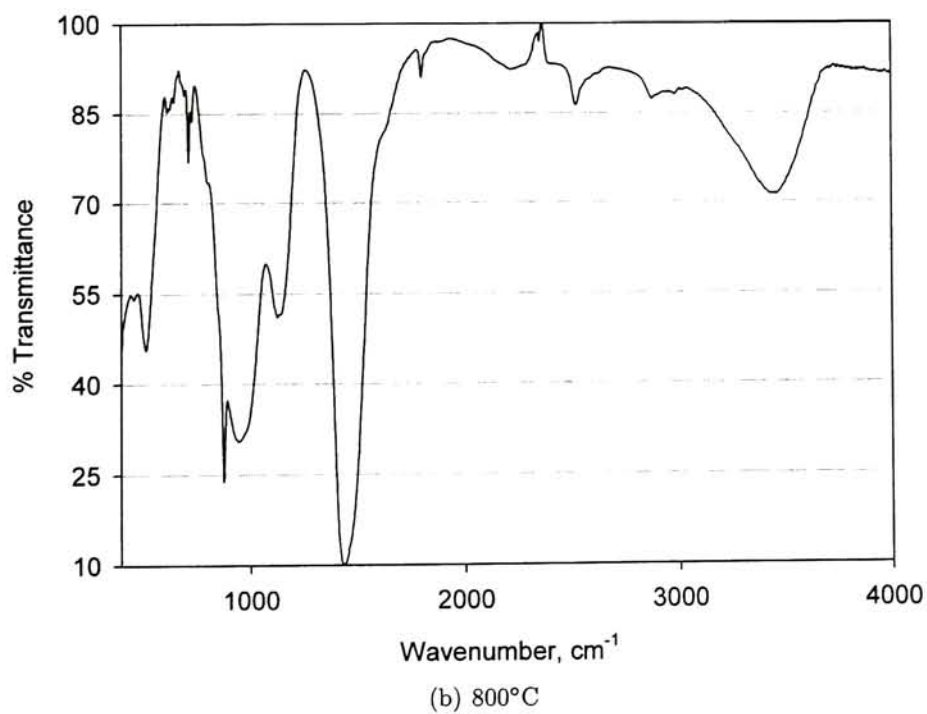
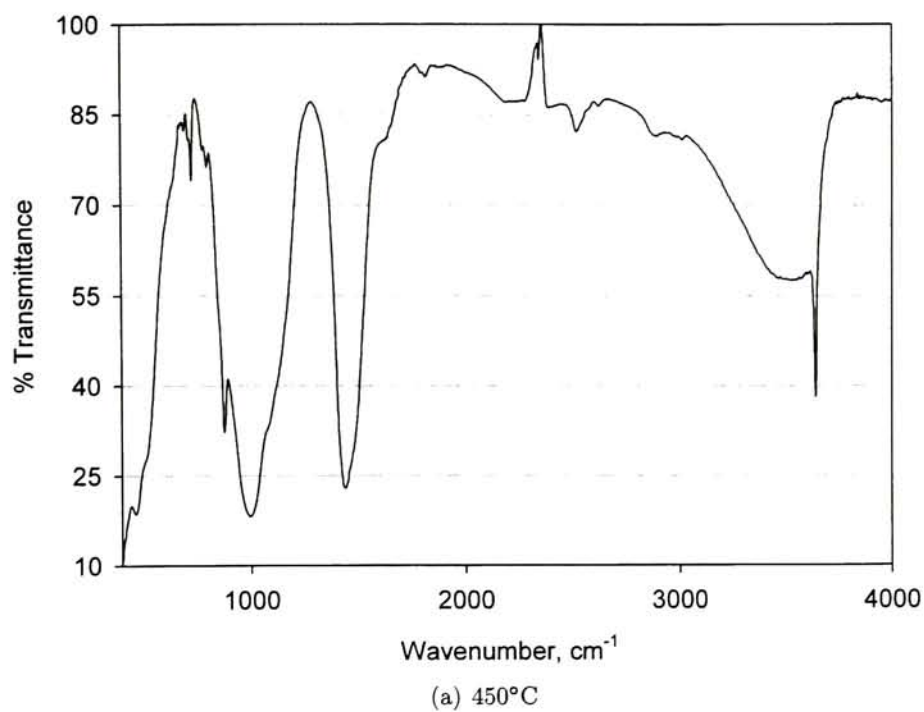


Figure 5.31: Infrared spectra of MKS-coated concrete exposed to 450°C and 800°C

Chapter 6

Conclusions and Suggestions for Future Work

6.1 Conclusions

The presented work focused on geopolymer characterization as well as proposed its application in the construction industry. Compressive strength tests showed that geopolymeric coatings based on metakaolin are effective thermal barriers that can be used to isolate concrete from high temperature environments. They exhibit better thermal stability than concrete up to 1000°C, which makes them perfect candidates for high temperature applications. Moreover, geopolymer properties can be tailored to fit specific project requirements, as their properties largely depend on starting materials and concentrations. This was successfully demonstrated through characterization of MK and MKS geopolymeric mixtures. Both compositions could be cured at room temperature or temperature as low as 65°C, providing for manufacturing process simplification. At the same time, they showed high degree of thermal and dimensional stability at temperatures of up to 800°C.

Based on the test results described in the previous chapter, it is recommended that metakaolin-based geopolymer with addition of amorphous silica be used as a protective coating for concrete. This recommendation is based on the following facts:

- Concrete samples containing amorphous silica showed minimal deterioration with increased temperature according to the thermogravimetric analysis. They retained a greater percentage of the original weight than did their metakaolin-based counterparts.
- Silica containing geopolymer expanded when subjected to elevated temperature, offering greater thermal insulation due to the presence of air voids.
- MKS geopolymer exhibited superior adhesion to concrete during the testing as compared to its metakaolin-based counterpart. This was true for samples exposed to any temperature of up to 800°C.
- Even though there were no significant differences between the two compositions of geopolymer based on the compressive strength measurements, MKS-coated mortar experienced the least amount of microstructural and chemical changes based on the infrared analysis and scanning electron microscopy studies. The final microstructure of these concrete samples resembled that of the unprotected cubes at room temperature.

6.2 Future Work

As with any research work, further experiments and testing need to be conducted to gain better understanding of the materials in question and to study their applications in the current industry. Some of the suggested improvements are outlined below:

- In the case of metakaolin-based geopolymer, an additive may need to be introduced to the geopolymer composition to prevent samples from developing cracks over time. Rheology changes may facilitate material handling through greater workability. Moreover, this may increase chemical binding of the coating to concrete, increasing its overall performance.
- Most of the published experimental results reviewed during the course of the project indicate several peaks on the infrared spectrum in the range of 400-600 cm^{-1} . However,

due to the equipment limitations it was not possible to observe and record any of those bands. Future work can focus on obtaining additional IR peaks in order to perform more complete characterization of geopolymeric materials used in this study. Such characterization, especially of MKS material, would be helpful for better understanding the process behind polymerization and protection offered by this material.

- One of the greatest problems encountered during the completion of this research was the inability to control the initial compressive strength of mortar. It is suggested that a method of preparing mortar cubes with uniform compressive strength be proposed for future studies. Such methods may involve the use of vibrating plates or similar devices with integrated timers to control the amount of load applied during the packing of mortar mixture into the molds.
- An additional in-situ monitoring of the compressive strength may be done on coated mortar cubes and unprotected samples to gain a better understanding of the changes in mechanical properties. This includes measuring the strength during the firing rather than after the samples have been cooled to the ambient temperature. Measurements taken in such a manner would provide a more precise set of data.
- Some of the future work may be focused on studying the interface of concrete and geopolymer and their interaction during the heat treatment process. Understanding the degree of surface adhesion, expansion, cracking, and other interactions may provide information on the benefits of one composition over the other. It may also help to explain the reason behind greater thermal protection offered by silica-containing samples than their metakaolin counterparts.
- It is important to ensure that MKS geopolymer will retain its adhesive and insulation properties over extended periods of time. It is believed that expansion and foaming effects are responsible for the higher level of thermal protection offered by the silica-

containing geopolymer. Consequently, these effects must be sustained for several years after the initial application in various environments.

Appendix A

Collected Data: Compressive Strength Measurements

Tables in this section present a summary of measured compressive strengths for mortar samples, coated and without any protection, at room temperature, 450°C, and 800°C. Each table corresponds to a particular set of samples. Prepared mortar cubes had dimensions of 2 x 2 x 2 in. Coating, if any, was removed before testing.

| | Unprotected | | | MK-coated | | MKS-coated | |
|---------------------|-------------|-------|-------|-----------|-------|------------|-------|
| | Room Temp. | 450°C | 800°C | 450°C | 800°C | 450°C | 800°C |
| 3950 | | 3138 | 1455 | 2825 | 2463 | 3474 | 2150 |
| 5003 | | 2200 | 1425 | 2981 | 2250 | 3172 | 1900 |
| 4000 | | 2520 | 1270 | 2498 | 2363 | 2555 | 2275 |
| 5010 | | 2550 | 1200 | 2870 | 2550 | 2544 | 2763 |
| 4855 | | 2163 | 1300 | 2980 | 2025 | 3285 | 2300 |
| 3475 | | 2300 | 1480 | 3443 | 2475 | 2842 | 2595 |
| 3835 | | 2950 | 1275 | 3732 | 2175 | 3640 | 1980 |
| 4768 | | | | | 2077 | 3452 | 1947 |
| 3860 | | | | | 1920 | 3297 | |
| 3915 | | | | | 2034 | 2847 | |
| 4555 | | | | | 1936 | | |
| 3925 | | | | | | | |
| 4835 | | | | | | | |
| 3875 | | | | | | | |
| 4283 | | | | | | | |
| 3495 | | | | | | | |
| 4443 | | | | | | | |
| 3565 | | | | | | | |
| 3568 | | | | | | | |
| 3805 | | | | | | | |
| 3771 | | | | | | | |
| Mean | 4133 | 2546 | 1344 | 3047 | 3111 | 2206 | 2239 |
| Standard Deviation | 516 | 374 | 108 | 412 | 390 | 228 | 312 |
| Coeff. of Variation | 12.5 | 14.7 | 8.1 | 13.5 | 12.5 | 10.3 | 13.9 |

Table A.1: Compressive strength (psi) of Unprotected, MK-, and MKS-coated mortar cubes at room temperature, 450°C and 800°C

Appendix B

Scanning Electron Microscopy and Infrared Analysis

This section presents a set of scanning electron microscope micrographs and infrared spectra described in previous chapters. The photographs and graphs are shown for comparison purposes. Larger images are given in the *Analysis and Discussion* section of this work.

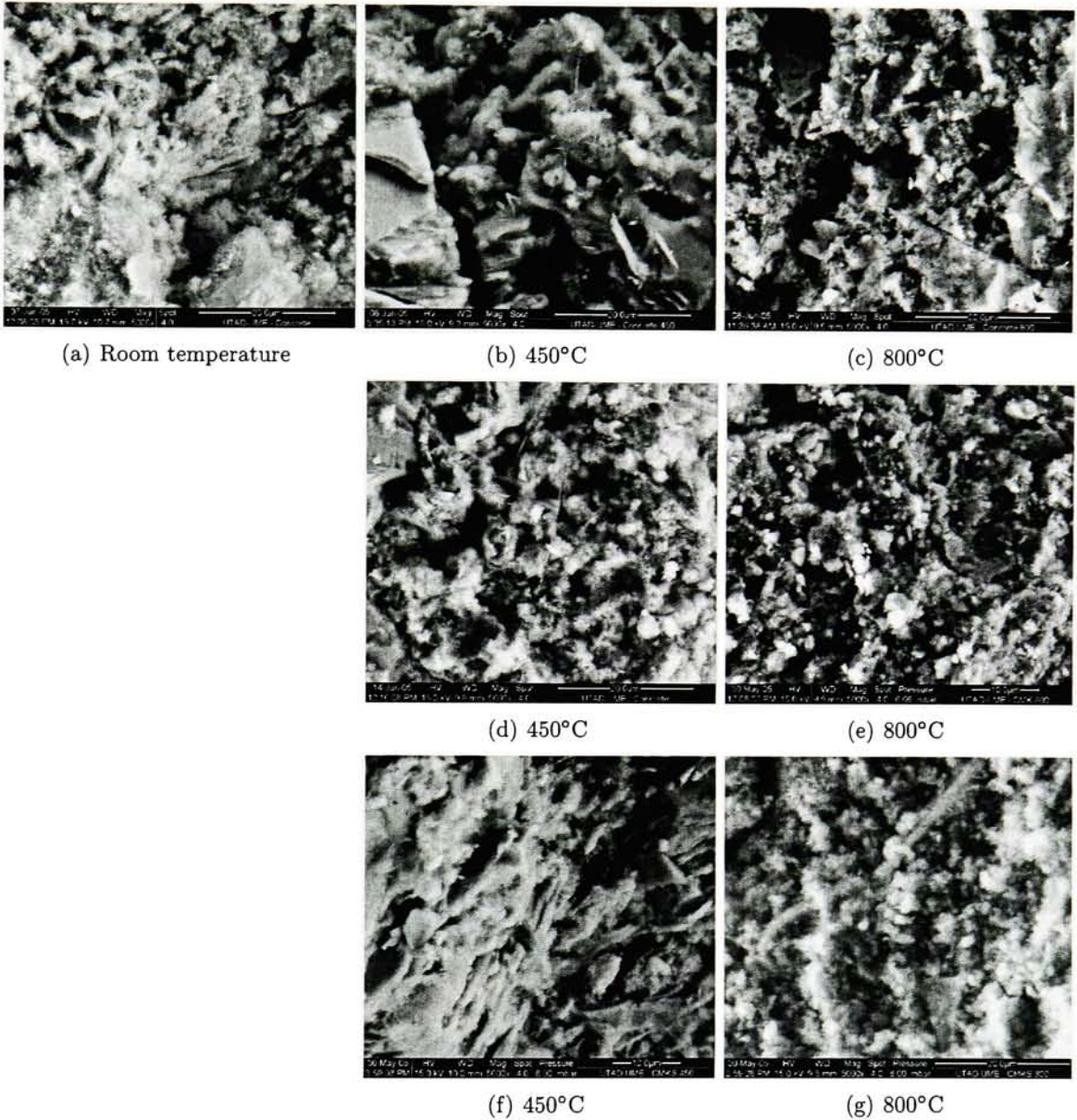


Figure B.1: Scanning electron microscope (SEM) micrographs of unprotected (a), (b), (c), MK-coated (d), (e), and MKS-coated (f), (g) mortar microstructure at room temperature and after exposure to 450°C and 800°C

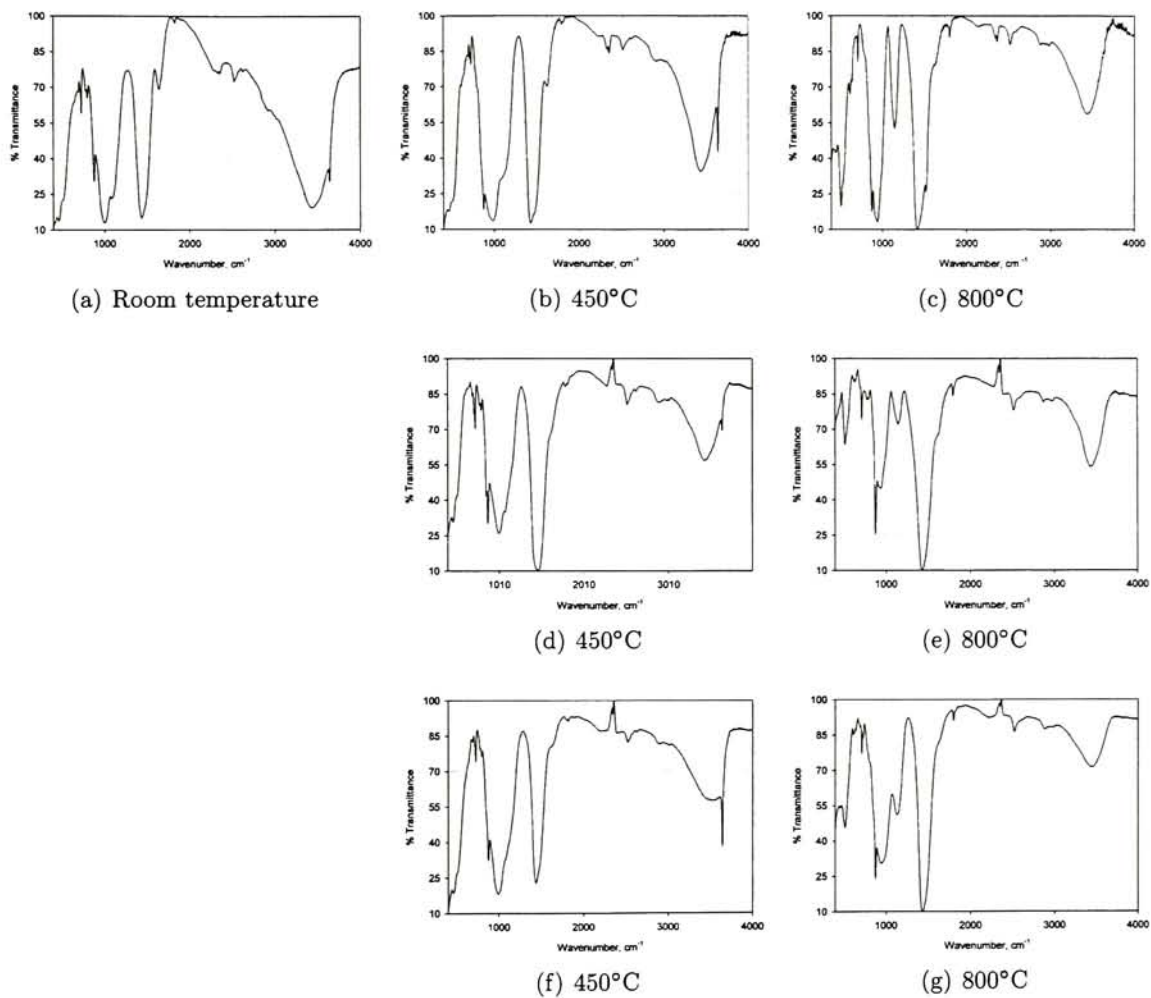


Figure B.2: Infrared (IR) spectra of unprotected (a), (b), (c), MK-coated (d), (e), and MKS-coated (f), (g) mortar at room temperature and after exposure to 450°C and 800°C

References

- [1] Arthur H. Nilson and George Winter. *Design of Concrete Structures*. McGraw Hill, 11th edition, 1991.
- [2] Theodore W. Marotta and Charles A. Herubin. *Basic Construction Materials*. Prentice-Hall, 5th edition, 1997.
- [3] C. B. Wilby. *Concrete Materials and Structures: a University Civil Engineering Text*. Cambridge University Press, 1991.
- [4] Benjamin Varela. *A Study of the Suitability of Geopolymers for Structural Steel Fire Protection*. PhD thesis, New Mexico State University, December 2002.
- [5] Joseph Davidovits. Geopolymers: Inorganic polymeric new materials. *Journal of Thermal Analysis*, 37:1633–1656, 1991. Reprinted by Geopolymer Institute, 1997.
- [6] Min Li; ChunXiang Qian; Wei Sun. Mechanical properties of high-strength concrete after fire. *Cement and Concrete Research*, 34:1001–1005, 2004.
- [7] Chi-Sun Poon; Salman Azhar; Mike Anson; Yuk-Lung Wong. Strength and durability recovery of fire-damaged concrete after post-fire-curing. *Cement and Concrete Research*, 31:1307–1318, June 2001.
- [8] Robert Park and William L. Gamble. *Reinforced Concrete Slabs*. John Wiley and Sons, Inc., 2nd edition, 2000.
- [9] Richard E. Lyon; P.N. Balaguru; Andrew Foden; Usman Sorathia; Joseph Davidovits; Michel Davidovics. Fire-resistant aluminosilicate composites. *Fire and Materials*, 21:67–73, 1997.
- [10] Djwantoro Hardjito; Steenie E. Wallah; Dody M.J. Sumajouw; B.V. Rangan. Geopolymer concrete: turn waste into environmentally friendly concrete. 2003.
- [11] Valeria F. F. Barbosa; Kenneth J. D. MacKenzie; Clelio Thaumaturgo. Synthesis and characterisation of materials based on inorganic polymers of alumina and silica: sodium polysialate polymers. *International Journal of Inorganic Materials*, 2:309–317, 2000.
- [12] Therese McAllister (editor). World Trade Center building performance study: Data collection, preliminary observations, and recommendations. FEMA 403, Federal Emergency Management Agency, May 2002.

- [13] Jesse Beitel and Nestor Iwankiw. Analysis of needs and existing capabilities for full-scale fire resistance testing. Nist gcr 02-843, National Institute of Standards and Technology, December 2002.
- [14] William D. Travers. Evaluation of the effects of the Baltimore tunnel fire on rail transportation of spent nuclear fuel. Technical report, U.S. Nuclear Regulatory Commission, January 2003.
- [15] Nabi Yüzer; Fevziye Aköz; Leyla Dokuzer Öztürk. Compressive strength - color change relation in mortars at high temperature. *Cement and Concrete Research*, 34:1803–1807, 2004.
- [16] B. Georgali and P.E. Tsakiridis. Microstructure of fire-damaged concrete. A case study. *Cement and Concrete Composites*, 27:255–259, 2005.
- [17] A.M. Neville. *Properties of Concrete*. John Wiley and Sons, 4th edition, 1996.
- [18] M. M. El-Hawary; A. M. Ragab; A. Abd El-Azim; S. Elibiari. Effect of fire on shear behaviour of R. C. beams. *Computers and Structures*, 65(2):281–287, 1997.
- [19] H. Weigler and R. Fischer. Influence of high temperature on strength and deformations of concrete. In Clyde E. Kesler, editor, *Concrete for Nuclear Reactors*, volume 1, pages 481–493. American Concrete Institute, 1972. Paper SP 34-26.
- [20] Yunsheng Xu and D.D.L. Chung. Improving silica fume cement by using silane. *Cement and Concrete Research*, 30:1305–1311, 2000.
- [21] Ki-Yeol Shin; Sang-Baik Kim; Jong-Hwan Kim; Mo Chung; Pyung-Suk Jung. Thermo-physical properties and transient heat transfer of concrete at elevated temperatures. *Nuclear Engineering and Design*, 212:233–241, 2002.
- [22] Kook-Han Kim; Sang-Eun Jeonb; Jin-Keun Kimb; Sungchul Yangc. An experimental study on thermal conductivity of concrete. *Cement and Concrete Research*, 33:363–371, 2003.
- [23] Waltraud M. Kriven; Jonathon L. Bell; Matthew Gordon. Microstructure and microchemistry of fully-reacted geopolymers and geopolymer matrix composites. *Ceramic Transactions*, 153:227–250, 2003.
- [24] Joseph Davidovits (1973). U.S. patent no. 3,950,470. Washington, DC: U.S. Patent and Trademark Office.
- [25] Joseph Davidovits (1982). U.S. patent no. 4,349,386. Washington, DC: U.S. Patent and Trademark Office.
- [26] Andrew James Foden. *Mechanical Properties And Material Characterization Of Polysialate Structural Composites*. PhD thesis, Rutgers The State University Of New Jersey - New Brunswick, 1999. Advisor: P. N. Balaguru; Accession No: AAG9918319.

- [27] Brian C. Smith. *Infrared Spectral Interpretation: A Systematic Approach*. CRC Press, 1999.
- [28] A. Palomo; M.T. Blanco-Varela; M.L. Granizo; F. Puertas; T. Vazquez; M.W. Grutzeck. Chemical stability of cementitious materials based on metakaolin. *Cement and Concrete Research*, 29:997–1004, 1999.
- [29] M.L. Granizo; M.T. Blanco-Varela; A. Palomo. Influence of the starting kaolin on alkali-activated materials based on metakaolin. study of the reaction parameters by isothermal conduction calorimetry. *Journal of Materials Science*, 35:6309–6315, 2000.
- [30] Puyam S. Singh; Tim Bastow; Mark Trigg. Outstanding problems posed by nonpolymeric particulates in the synthesis of a well-structured geopolymeric material. *Cement and Concrete Research*, 34:1943–1947, 2004.
- [31] Amandio Teixeira Pinto and Eduardo Vieira. Optimised conditions for the obtaining of metakaolin. To be published in Materials Science Forum.
- [32] A. Burl Donaldson and Benjamin Varela. Evaluation of the curing kinetics for a geopolymer using differential scanning calorimetry. In *NATAS Annual Conference*, Albuquerque, NM, September 22-24 2003.
- [33] T. Bakharev. Resistance of geopolymer materials to acid attack. *Cement and Concrete Research*, 35:658–670, 2005.
- [34] S. Alonso and A. Palomo. Alkaline activation of metakaolin and calcium hydroxide mixtures: Influence of temperature, activator concentration and solids ratio. *Materials Letters*, 47:55–62, 2001.
- [35] A. Teixeira-Pinto; P. Fernandes; S. Jalali. Geopolymer manufacture and application - main problems when using concrete technology. In *Geopolymers 2002*, Hotel Sofitel, Melbourne, Australia, October 2002.
- [36] Valeria F.F. Barbosa and Kenneth J.D. MacKenzie. Thermal behavior of inorganic geopolymers and composites derived from sodium polysialate. *Materials Research Bulletin*, 38(2):319–331, January 2003.
- [37] Joseph Davidovits (1984). U.S. patent no. 4,472,199. Washington, DC: U.S. Patent and Trademark Office.
- [38] A. Palomo; A. Macias; M.T. Blanco; F. Puertas. Physical, chemical and mechanical characterization of geopolymer. In *9th International Congress on the Chemistry of Cement*, 1992.
- [39] Joseph Davidovits. Properties of geopolymer cements. In P.V. Krivenko, editor, *First International Conference on Alkaline Cements and Concretes*, volume 1, pages 131–149, Kiev, Ukraine, 1994. Kiev State Technical University, Kiev, Ukraine.
- [40] Valeria F. F. Barbosa and Kenneth J. D. MacKenzie. Synthesis and thermal behaviour of potassium sialate geopolymers. *Materials Letters*, 57:1477–1482, 2003.

- [41] ECC International. China clay (kaolin). <http://www.ecci.co.uk/ceramics/>, June 21 2005.
- [42] PQ Corporation. Sodium silicate - products and specifications. <http://www.pqcorp.com/productlines/sodiumsilicatespecs.asp>, June 21 2005.
- [43] Standard test method for compressive strength of hydraulic cement mortars (using 2-in or [50-mm] cube specimens). In Sean J. Bailey et al., editor, *Annual Book of ASTM Standards*, volume 04.01: Cement; Lime; Gypsum of *Section 4: Construction*. ASTM International, 2003.
- [44] Theodore L. Brown; H. Eugene LeMay; Bruce E. Bursten. *Chemistry: the Central Science*. Prentice-Hall, 8th edition edition, 2000.
- [45] George Socrates. *Infrared and Raman Characteristic Group Frequencies: Tables and Charts*. John Wiley and Sons, Ltd., 3rd edition, 2001.
- [46] Richard A. Nyquist and Ronald O. Kagel. *Infrared Spectra of Inorganic Compounds*, volume 4. 1997.
- [47] John W. Phair; Jannie S. J. Van Deventer; J. David Smith. Mechanisms of polysialation in the incorporation of zirconia into fly ash-based geopolymers. *Ind. Engineering Chemical Research*, 39(8):2925–2934, 2000.
- [48] W. K. W. Lee and J. S. J. van Deventer. The effects of inorganic salt contamination on the strength and durability of geopolymers. *Colloids and Surfaces A: Physicochemical Engineering Aspects*, 211:115–126, 2002.
- [49] National Institute of Standards and Technology. NIST chemistry webbook. <http://webbook.nist.gov/chemistry/>, March 8 2005.
- [50] S. Bruni; F. Cariatia; P. Fermoia; A. Pozzia; L. Toniolo. Characterization of ancient magnesian mortars coming from northern italy. *Thermochimica Acta*, 321:161–165, 1998.
- [51] Xi-Shu Wang; Bi-Sheng Wu; Qing-Yuan Wang. Online sem investigation of microcrack characteristics of concretes at various temperatures. *Cement and Concrete Research*, 35:1385–1390, 2005.
- [52] S.K. Handoo; S. Agarwal; S.K. Agarwal. Physicochemical, mineralogical, and morphological characteristics of concrete exposed to elevated temperatures. *Cement and Concrete Research*, 32:1009–1018, 2002.